Review

Effects of Shot Peening Treatment on the Properties of Additive and Conventionally Manufactured Ti6Al4V Alloy: A Review

Wojciech Okuniewski , Mariusz Walczak * , Mirosław Szala *

Posted Date: 18 January 2024

doi: 10.20944/preprints202401.1375.v1

Keywords: additive manufacturing; shot peening; Ti-6Al-4V; peening; titanium alloy; mechanical properties; surface engineering; electropolishing.

Review

Effects of Shot Peening Treatment on the Properties of Additive and Conventionally Manufactured Ti6Al4V Alloy: A Review

Wojciech Okuniewski, Mariusz Walczak * and Mirosław Szala *

Department of Materials Engineering, Faculty of Mechanical Engineering, Lublin University of Technology, Nadbystrzycka 36D, 20-618 Lublin, Poland; wojciech.okuniewski@pollub.edu.pl

* Correspondence: m.walczak@pollub.pl. (M.W.); m.szala@pollub.pl (M.S.)

Abstract: Literature review indicates that the basic microstructure of Ti-6Al-4V is bimodal which consist of two phases: $\alpha + \beta$, and it occurs after the fabrication in conventional methods such as casting, plastic forming or machining processes. After the additive manufacturing methods, there could be significant changes in the microstructure. Due to the rapid heat exchange during heat-treatment process, bimodal microstructure transforms into lamellar microstructure which consists of two phases $\alpha' + \beta$. Despite applying optimum printing parameters, 3D-printed products exhibit typical surface defects and discontinuities. Recently, two of the primary technologies for the improvement of surface layer properties of titanium alloys are shot peening and electropolishing. Literature review signalizes that shot peening and electropolishing processes have positive impact on the corrosion behaviour, mechanical properties and the condition of the surface layer of titanium alloy. Furthermore, there is a lack of studies about combining shot peening and electropolishing in one hybrid process on titanium alloys, which could synthesize the benefits of both processes. The scope of future investigation is also included in this review.

Keywords: additive manufacturing; shot peening; Ti-6Al-4V; peening; titanium alloy; mechanical properties; surface engineering; electropolishing

1. Introduction

Nowadays, the demand for improving materials from titanium alloys has increased tremendously. The reason for this is that titanium alloys are characterised by low density, high specific strength, corrosion resistance and good process performance with wide applications in the world economy in industries such as aerospace, marine, automobile, biomedical, chemical, energy and many others [1–3]. In evidence, in Figure 1. there are shown results from research centres of Web of Science and Scopus and the number of articles on the subject of shot penning, additive manufacturing, Ti-6Al-4V titanium alloy.

As it can be observed from Figure 1, Additive Manufacturing is a prominent subject of the today's studies. In addition, it is worth noting that these numbers only include Additive Manufacturing phrase. There are definitely more articles which use specific AM terminology like SLM, DMLS or its full names without mentioning the phrase Additive Manufacturing or AM abbreviation. Noteworthy is also the fact that there are numerous studies about shot peening treatment which means that this type of surface treatment is still to be fully exploited. Moreover, it can be observed that even though recent reports suggest an increase interest in new β-phase titanium alloys, Ti-6Al-4V titanium alloy is continuously considered as a valuable subject of the research.

Preprints (www.preprints.org) | NOT PEER-REVIEWED | Posted: 18 January 2024 doi:10.20944/preprints202401.1375.v1

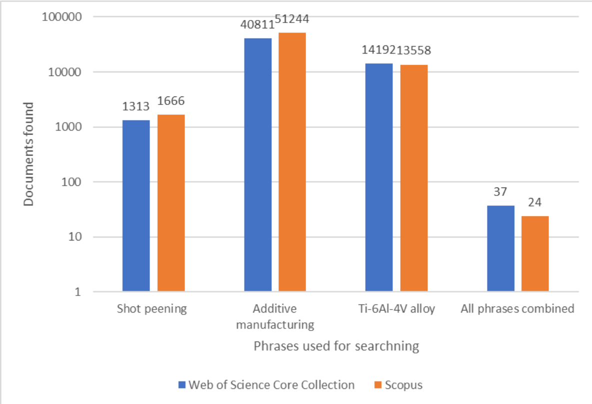

Figure 1. Searching results for selected phrases relating to papers scope. Search done in title, abstract and keywords of papers published in years 2019-2023, and indexed in Web of Science Core Collection and Scopus.

Increased interest in titanium alloys is caused by many factors. One of the examples can be seen in medical applications: world societies focus more on their health and start being more active. That results in much younger patients, who do not want to change their lifestyle and place more physical strain on the implants. It means that implants have to serve longer with more efficiency [4]. The quality of implants is crucial because as wear and corrosion processes contribute negatively on the properties of the implant, they might also have a direct negative biological impact on the periprosthetic environment [5,6]. Table 1 shows a comparison of widely used materials in biomedical applications in terms of their physicomechanical properties.

Table 1. Comparison of physicomechanical properties of popular biomedical materials: Ti6Al4V alloy, 316 L stainless steel, CoCrMo alloys to natural cortical human bone [7–10].

Properties	Natural Human Bone	Ti6Al4V Alloy (wrought)	316L Stainless Steel (cast)	F75CoCrMo Alloy (cast)
Density (g/cm³)	1.5-2	4.4	8.0	8.8
Tensile modulus of elasticity (GPa)	-	830-1070	205	500-1500
Yield Strength (MPa)	130-190	920-1140	515	900-1800
Ultimate tensile strength (MPa)	10-30	100-110	195-205	200-230
Elongation (%)	-	10-15	10-40	4-13

Titanium alloys are very sensitive to surface integrity, which is directly related to their performance. This generates the need of surface treatment of Ti-6A1-4V components in engineering in order to improve the surface integrity. The well-established post-producing surface treatment technologies for modifying surface layer of Ti-6Al-4V are shot peening and electropolishing [11,12]. There are numerous studies which indicate that combining those technologies on steels is profitable [13,14]. However, there is very little information about the impact on titanium alloys, especially, on additively manufactured Ti-6Al-4V titanium alloy. So, the main purpose of this review is to summarize all of the gathered data about the influence of shot peening and electropolishing processes on Ti-6Al-4V titanium alloy as well as gather information from the literature data about the influence of combined treatments of shot peening and electropolishing.

Preprints (www.preprints.org) | NOT PEER-REVIEWED | Posted: 18 January 2024 doi:10.20944/preprints202401.1375.v1

2. Properties of Ti6Al4V Manufactured Using Conventional Methods and Additive Manufacturing Methods

2.1. Microstructural Phases

Conventional microstructure of titanium alloys can be structurally classified by the size and organization of dual-phase α and β. Titanium alloys usually experience thermomechanical treatments [15]. Ti–6Al–4V contains 6% of aluminium element, which stabilizes hexagonal close-packed α-phase, and 4% of vanadium element, which stabilizes β-phase. Both phases i.e., α phase (hcp) and β phase (bcc), coexists at room temperature [16]. The control and the optimization of the microstructure of Ti-6Al-4V alloy is one of the most important issues to achieve desired properties. During the heating process, α-phase transforms into β phase approximately at temperature 1000 °C and it is called β transus temperature (Tβ). The heat treatment below β transus is referred to as sub-transus whereas above β transus is referred to as super-transus [17]. The cooling rate determines the transformation of β into → α (α′)(α″). The transformation of unit cells is shown on Figure 2 Results

This section may be divided by subheadings. It should provide a concise and precise description of the experimental results, their interpretation, as well as the experimental conclusions that can be drawn.

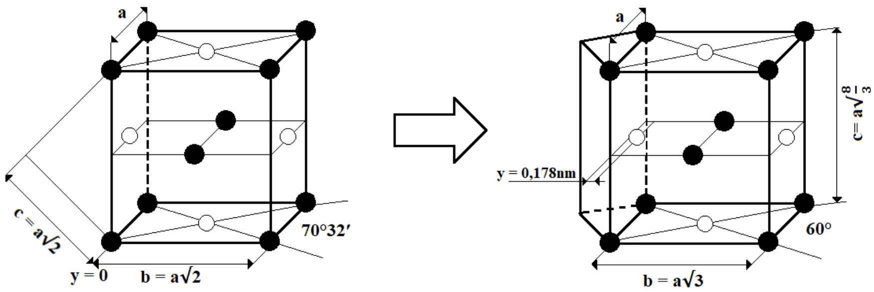

Figure 2. Martensitic transformation of unit cells in Ti6Al4V: β phase (a), α and α′ phases (b) based on [18,19].

The basic microstructure of Ti6Al4V alloy is bimodal of interconnected equiaxed primary α grains and lamellar α+β colonies (transformed β). An example of this structure shows Figure 3a. On the other hand, martensitic structure is lamellar, which can be obtained as a Widmanstätten structure (Figure 3b) [20] or martensite plates.

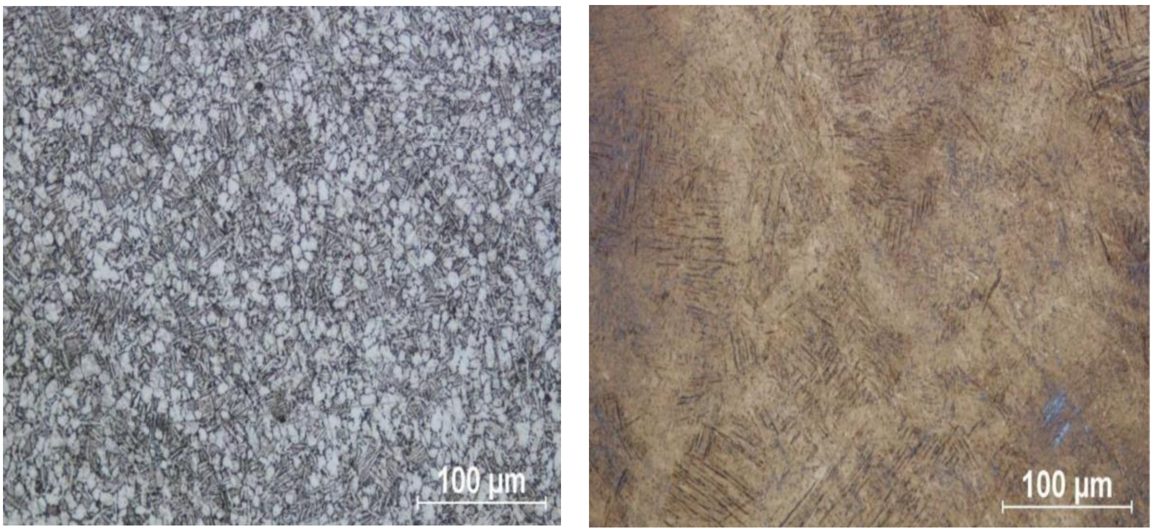

(**a**) (**b**)

Figure 3. Micrographs of the microstructures of Ti-6Al-4V: (**a**) bimodal (basic microstructure) (**b**) lamellar (martensitic microstructure) [20].

Martensitic two-phase $\alpha + \beta$ alloys in the hardened state depends on the quenching temperature. The phase constituents could be in the form of martensitic phase precipitations of the α' and α_M, as well as grains of metastable β_M phase [18]. The scheme of emerging phases depending on the cooling rate is shown in Figure 4.

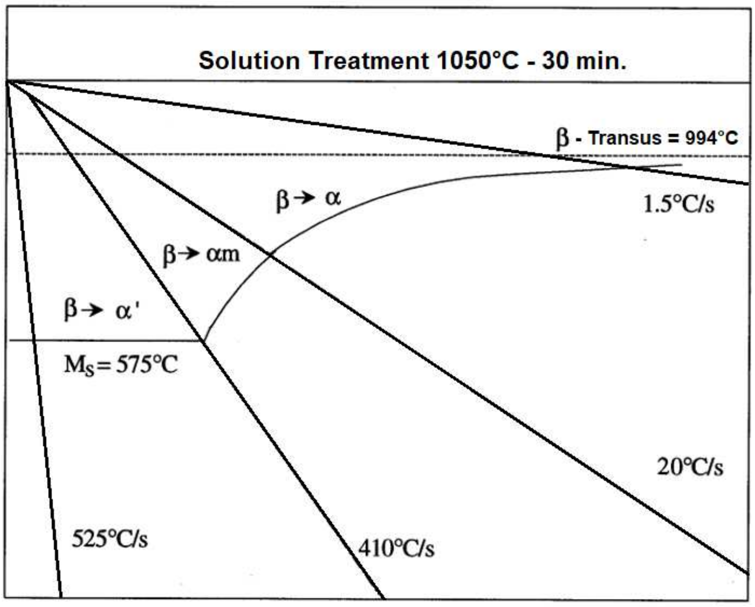

Figure 4. Schematic continuous cooling diagram for Ti–6Al–4V β-solution treated at 1050°C for 30 min [21].

The impact on microstructure has also cooling medium which then results in differences in Ti6Al4V properties. Table 2 describes the expected microstructure which is classified according to the cooling medium used and the phases in which the transformation occurs, irrespective of the material soaking time [22].

Table 2. The microstructure of Ti6Al4V under phase transformation and different cooling medium [22].

Phase Transformation Region	Temperature Range (°C)	Microstructure at various cooling medium		
		Water	Air	Furnace
$\alpha + \beta$	700-950	A mixture of α and β structures, with more volume of α structures	Primary α, with grains having $\alpha + \beta$ lamellar structure	Primary α phase with intergranular β phase observed for all temperatures α phase on the phase boundary and a transition from β to α on the grain boundary. The grains were observed to have α/
β	950-1100	Martensite microstructure consist of a fine acicular α phase with grain boundaries consisting of β phase	Partial martensitic microstructure, there exists an incomplete transition from β to α phase on grain boundaries	

Preprints (www.preprints.org) | NOT PEER-REVIEWED | Posted: 18 January 2024 doi:10.20944/preprints202401.1375.v1

	β lamellar

2.2. Manufacturing Methods of Ti6Al4V Martensitic Structure

2.2.1. Subtractive Manufacturing

Transformation of basic α+β into martensitic α'+ β could be made in conventional heat-treatment processes: quenching and annealing. In industry applications, the combination of solution heat-treatment and ageing operation is used in aerospace and automobile industry [23]. The main reason is that microstructure consists of soft α-phase and grain boundary β [24]. The effect on mechanical properties of Ti6Al4V is shown in Table 3

Table 3. Mechanical properties after different SM methods of Ti6Al4V [25–29].

Process	Heat Treatment of Ti6Al4V alloy	Microstructure at various cooling medium				Ref.
		Microhardness	**Yield Strength [MPa]**	**Ultimate Tensile Strength [MPa]**	**Elongation [%]**	
Wrought	Untreated	325 HV	880	960	14	[25]
	Untreated	190 HK	880	910	18	[26]
	Ti6Al4V water quenching + aging	320 HK	1110	1170	6,5	[26]
	Ti6Al4V air cooling+aging	210 HK	910	980	12,5	[26]
Forged	Mill annealed	-	1030	970	16	[27]
	Mill annealed	-	960	1006	18,37	[25]
Cast	-	330 HV	750	875	4,5	[28]
	-	-	865	980	13,5	[29]

However, the conventional methods (CM) are slowly being replaced by additive manufacturing methods (AM). The main reason for that is hard machining material which is caused by the low thermal conductivity. There are certain challenges in refining casting, forging or rolling leading to notable amount of material waste, long lead time and high fabricating cost [30]. As a solution to this challenging scenario, additive manufacturing gained attention as it has immanent advantages, such as unrivalled design freedom and short lead times [31]. The extensive researches in this area implicate that achievable characteristics of Ti6Al4V are satisfying [32] and even could be superior for certain characteristics, like ductility [33].

2.2.2. Additive Manufacturing

There are 7 main powder bed technologies as per ASTM F2792 norm shown in Figure 5 [32]

Preprints (www.preprints.org) | NOT PEER-REVIEWED | Posted: 18 January 2024 doi:10.20944/preprints202401.1375.v1

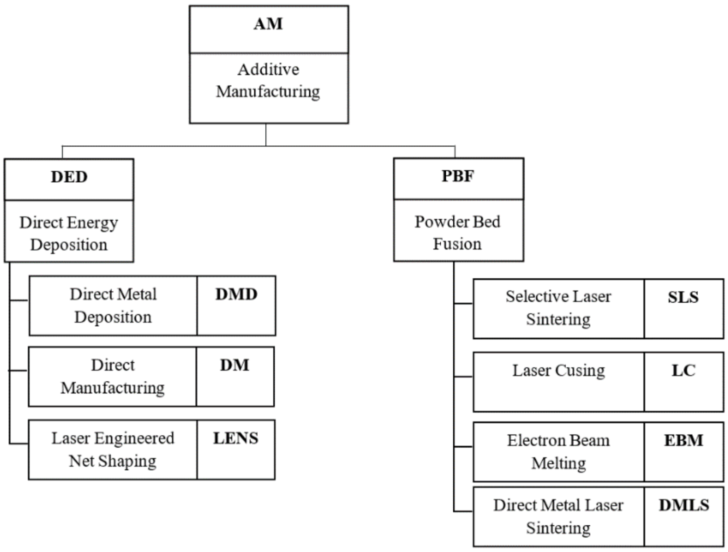

Figure 5. Powder based AM methods according to ASTM F2792 based on [32].

The power of the laser and the feed rate of powder have direct impact on homogeneity of additively manufactured structure [34]. The laser beam can be described as Gaussian moving heat source as Equation (1):

$$Q_{laser} = \frac{2Ap_{laser}}{\Pi r_0^2} \exp\left(\frac{-2(x_i - x_0 - v_{laser}t)^2}{r_0^2}\right) \quad (1)$$

where A is the laser absorption coefficient, P_{laser} is the laser power, r_0 is the focus radius, x_0 is the laser's beginning beam location, x_i is the position of laser focus, and v_{laser} is the laser's scanning speed, and the heat transfer equation according to Fourier's law can be described as (2) [35]:

$$Q_{laser} = \rho_m C_m \left(\frac{\partial T}{\partial t} + u\cdot\nabla T\right) - \nabla\cdot(\lambda \nabla T) \quad (2)$$

where ρ_m is the density, C_m is the specific heat, λ is the base thermal, conductivity, and u is the fluid flow velocity.

Literature indicates that powder bed fusion (PBF) technologies are used for industrial manufacturing of Ti6Al4V alloys [36,37]. In Table 4. comparison of the properties between particular PBF AM technologies and Direct Energy Deposition (DED) technology is presented.

Table 4. Comparison of mechanical properties of Ti6Al4V after manufacturing with particular AM technologies [27,38–50].

AM Technology	Specimen Orientation and Ref.		Mechanical Properties				
			Young Modulus [MPa]	Microhardness	Yield Strength [MPa]	Ultimate Tensile Strength [MPa]	Elongation [%]
DED	XZ	[38]	-	-	522	797	1,7
	XY	[38]	-	-	892	911	6,4
	XZ	[27]	-	-	945	1041	14,5
	XZ	[27]	-	-	970	1087	13,6
	XY	[39]	-	-	960	1063	10,9
SLM	XZ	[40]	115	-	978	1143	11,8
	ZX	[40]	119	-	967	1117	8,9
	XY	[40]	113	-	1075	1199	7,6
	XY	[41]	-	394 HV	1052	1136	2,92

 doi:10.20944/preprints202401.1375.v1

	XY	[42]	-	370 $HV_{0.3}$	1273	1421	3,2
	XZ	[42]	-	390 $HV_{0.3}$	1150	1246	1,4
	XY	[43]	-	350 HV	-	1137	9,10
EBM	XY	[44]	118	321 HV	830	915	13,1
	XY	[45]	114	35 HRC	830	914	13,1
	XY	[42]	-	315 $HV_{0.3}$	846	976	15,0
	XZ	[42]	-	340 $HV_{0.3}$	845	972	14,2
	ZX	[46]	-	-	869	965	-
DMLS	ZX	[46]	-	380 HV	1017	1096	16
	ZX	[47]	111,9	871 HV10	1086	1121	16,9
	XY	[48]	110	400-430 HV	1140	1290	7
	XY	[49]	-	-	990	1045	14
	ZX	[50]	108,0	-	982	1080	14,3
	XZ	[50]	108,7	-	980	1072	14,1

2.2.3. SLM—Selective Laser Melting

During the SLM process, a product is formed by selectively melting successive layers of Ti–6Al–4V powder by the interaction of a laser beam. The powder material is heated and after applying sufficient power, it melts and forms a liquid pool. The molten pool consolidates and cools down quickly [51]. During the cooling down process, decomposition of β-phase proceeds into diffusionless martensitic α' [52]. Afterwards, the cross-section of a layer is scanned, the building platform is lowered by an amount equal to the layer thickness and the process continues until the final product is formed [51]. Figure 6. shows scheme of SLM process.

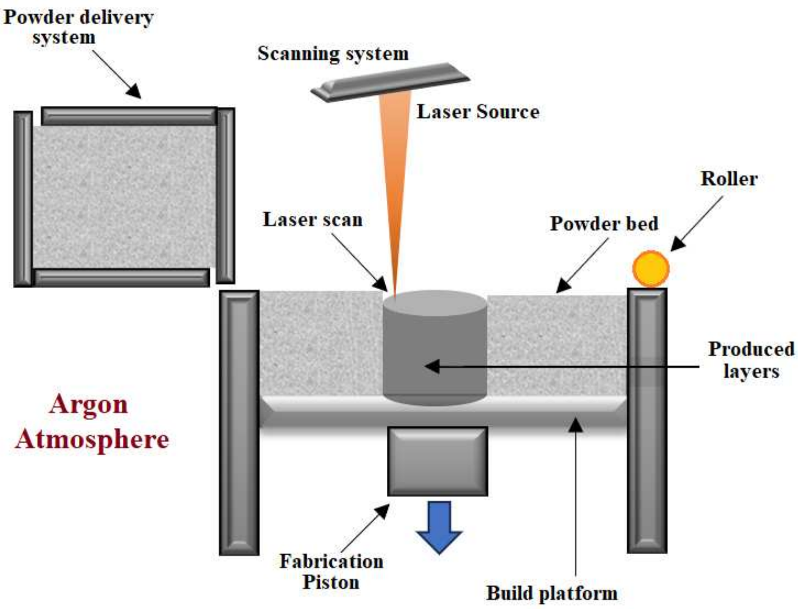

Figure 6. Diagram of the process of Selective Laser Melting according to [19,53].

Due to the high reactivity of Ti alloys, the process needs to be carried under an inert argon atmosphere [51]. SLM possesses several advantages such as a high material use efficiency, a high level of flexibility and production of geometrically complexed shape of parts, close to the final product [54]. The main disadvantages are mainly: higher cost, large residual stresses caused by steep thermal gradients and defects such as in conventional manufacturing like deformation [54] delamination [55], porosities [56] or even cracking of the parts in the form of hot cracking [57] or initiated by micro-sized defects [58].

2.2.4. DMLS—Directive Metal Laser Sintering

During the DMLS process, a moderately low intensity of laser power is used to sinter but not fully melt the metallic powders of Ti-6Al-4V alloy like in SLM process. DMLS process is initiated with placing a titanium alloy powder layer on the substrate, kept on the building platform, and then the laser beam is allowed to scan over the entire surface of the powder layer. The laser fuses the powder selectively or partially melts it in this process and then the powder bed is solidified to form a dense component [59,60]. Further, the platform is lowered down by a distance equal to layer thickness. A fresh layer of powder is again placed and the method is repeated in the same manner to get the final product [61]. The heat treatment and high cooling rate lead to the formation of dendritic martensite or fully acicular α' martensite in Ti6Al4V titanium alloy [62]. Figure 7. shows the scheme of the DMLS process.

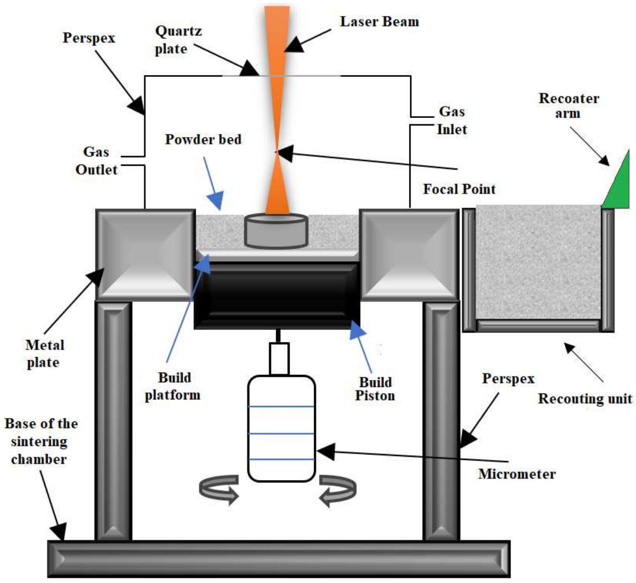

Figure 7. Schematic diagram of the DMLS process according to [63,64].

DMLS operation needs very careful observation since the occurrence of melting, re-solidification, heat transfer mechanism (convection, radiation) and volume shrinkage make it more challenging [65]. Process defects such as pores, cracks, high residual stresses and other microstructural defects can be noticed in DMLS operation [66].

2.2.5. EBM—Electron Beam Melting

During the EBM process, the electron beam or focused laser are the heat sources applied to melt the titanium powder. Each layer is manufactured by the following steps: spreading the titanium powders on a base plate, preheating of the powder, sintering of the powder with a defocused beam, melting the powders by using a focused beam, and then lowering the building platform by the thickness of one layer [67,68]. Using the electron beam necessitates the powder to be sintered or, otherwise, the electrostatic forces lead to clouds of charged particles in the build chamber [69]. The entirety of the EBM fabrication process operates under a vacuum environment. This implies that highly reactive materials, such as titanium alloys, can be produced using the EBM method, without oxidation and contamination of the parts throughout the process [70]. Figure 8. shows the scheme of the EBM process.

 doi:10.20944/preprints202401.1375.v1

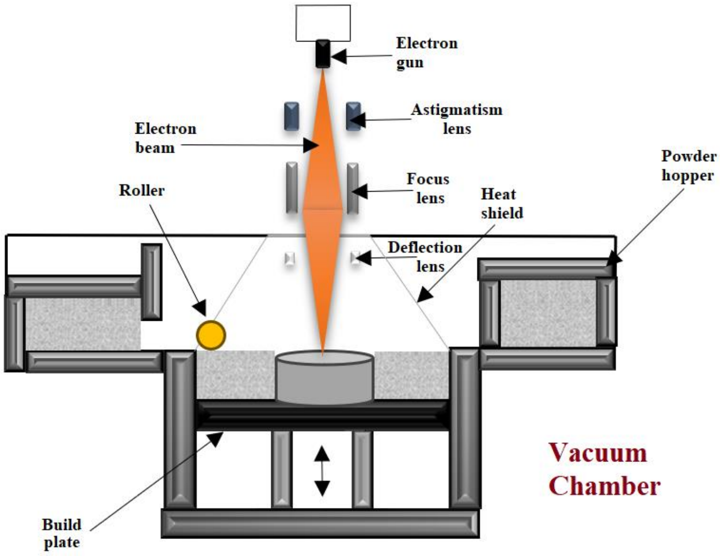

Figure 8. Schematic diagram of the EBM technique according to [71,72].

The defects after EBM manufacturing process are similar to the defects after other AM technologies. There are different types of defects after EBM producing Ti-6Al-4V titanium alloy, which have different origins in the building process [73]. Distinct defect types show differences in both size and shape, which are the factors that influence crack initiation behaviour. Lack of fusion defects are also common anomalies which are a result of under-melting during processing [74–76]. On the other hand, porosity is a result of over-melting during production and partially vaporizing the titanium metal [76,77]. Another defect type is gas pores which are coming from the powder or the building process. Many defect types can be avoided or minimized by appropriately selected processing parameters, but gas pores are generally considered unavoidable [78]. Population of these defects has direct influence on fatigue life of EBM produced Ti-6Al-4V titanium alloy [79].

2.2.6. DED—Direct Energy Deposition Processes

During Direct Energy Deposition (DED) a stream of metallic powder or wire is fed into a melt pool that is created by a laser beam and melts it as it is deposited [80]. It varies from Powder Bed Fusion technologies (PBF) where thermal energy is used to selectively fuse regions of a powder bed. Main application of DED processes are typically used on existing parts of arbitrary geometry with a relatively high deposition rate [81]. During the DED process, the electron or laser beam creates a molten pool on the surface. Then, the material transfer is conducted using a nozzle (laser as powder and beam as wire). The nozzle and the beam move along the path determined by the CAD data. The consecutive layers are melted and frozen on each other until the process is completed. The whole process takes place in a chamber filled with inert gas when using the laser method or vacuum environment when electron beam is used [67,82–86]. The scheme of building layers in DED technology using laser is shown in Figure 9.

Preprints (www.preprints.org) | NOT PEER-REVIEWED | Posted: 18 January 2024 doi:10.20944/preprints202401.1375.v1

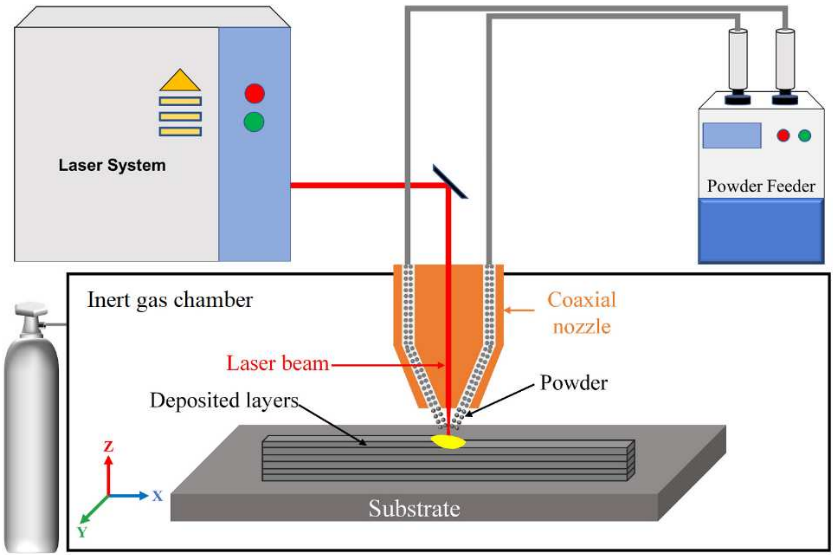

Figure 9. Schematic diagram of the DED process using laser beam [87]. Copyright Elsevier, 2024.

It has been well established that products of DED technology cannot be completely free from defects (i.e., pores, un-melted powder and Lack of fusion (LOF)). LOFs are developed when the molten material in one layer does not completely fill the space between each DED pass, forming crack-like features perpendicular to BD [88–91]. Other typical defects after DED process are shrinkage, residual stresses and deformations after local temperature difference occurring, which means post-fabrication machining is often required. Utilizing wires and metallic sheets as printing feedstock material in DED processes usually lead to more defects, lower geometry precision, high surface roughness and limitations for the production of complex shapes rather than using powder feedstock in PBF technologies However, often better static and dynamic mechanical properties are obtained in the DED-deposited condition rather than in PBF-deposited parts [92–94].

3. Post-Process Surface Treatment Methods Applied to Modifying Ti6Al4V Surface Layer

3.1. Post-Processing after Additive Manufacturing

Metal parts fabricated directly by additive manufacturing are usually not ready for the service in their as-built state. Once the building process is completed, parts often have to be subjected to post-processing treatment including support material removal, surface finishing, colouring, coating and heat treatment. Existing heat treatment standards for CM metals and alloys are not specifically designed for AM parts and may differ in many cases depending on the initial microstructures and desired properties for specific applications. That is why it is crucial to determine optimal parameters of the post-processing treatment as it would not only improve properties of this materials but also be beneficial in reducing the cost of the process [95]. However, the application of optimal 3D-priniting parameters recommended by the producers does not avoid exhibition of surface defects, anomalies and undesired residual stresses in Ti-6Al-4V products. These lead to unsatisfactory properties for their application and are a justification for the use of surface finishing treatment like the shot peening process [96]. The scheme of a typical surface layer after AM is shown in Figure 10, and SEM microphotographs, illustrating the morphology of specimens surface after AM technology of DMLS, is shown Figure 11

 doi:10.20944/preprints202401.1375.v1

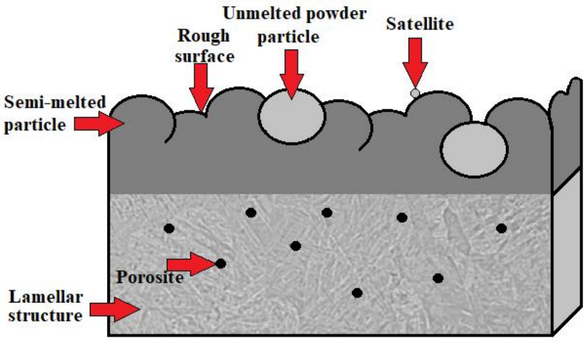

Figure 10. Schematic illustration of surface defects and anomalies after Additive Manufacturing [97–99].

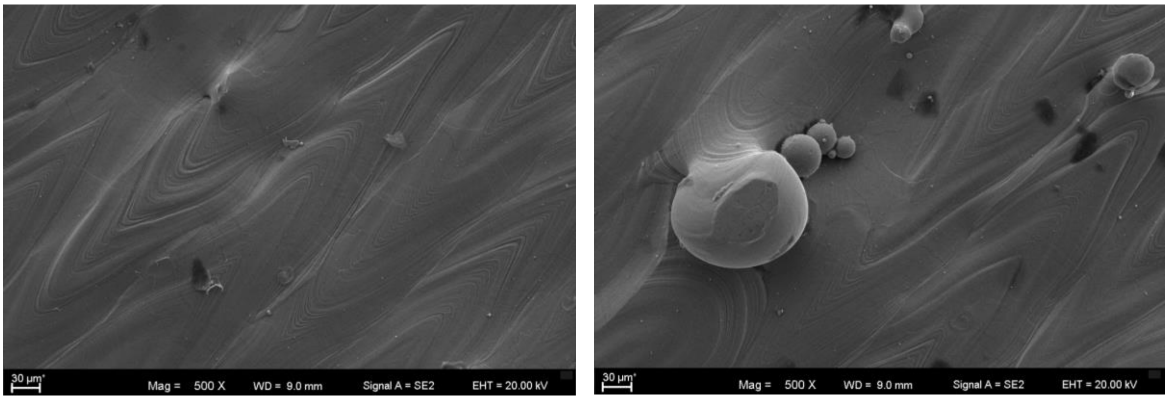

(**a**) (**b**)

Figure 11. Typical surface defects and discontinuities: (**a**) collapse of the welding pool; (**b**) partially melted titanium powder [100].

3.2. Shot Peening

One of the most popular methods of modifying the surface layer is shot peening (SP). Shot peening is a mechanical surface treatment performed by the repeated impact of shots at high impact velocities onto surfaces of materials which causes plastic deformation of this material [101]. The amount of the plastic deformation of shot peening process influences failure mechanisms such as fatigue [102–104] and corrosion [105]. It also has an impact on important mechanical properties of material such as surface roughness [106], hardness [107] and residual stresses [108]. The scheme of the effect of shot peening process is shown on Figure 12 and modified structure of surface layer obtained after the process is shown on Figure 13.

Preprints (www.preprints.org) | NOT PEER-REVIEWED | Posted: 18 January 2024 doi:10.20944/preprints202401.1375.v1

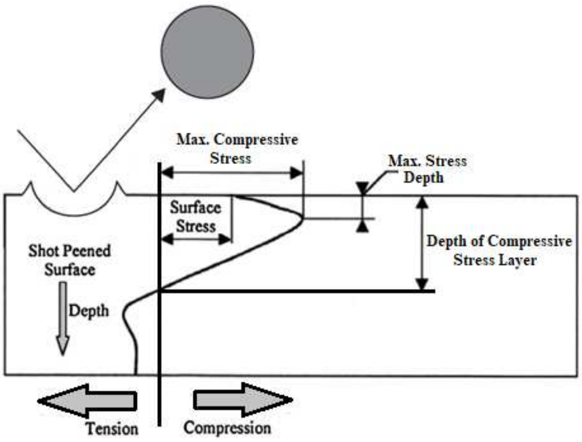

Figure 12. Effects of shot peening process according to [4,109].

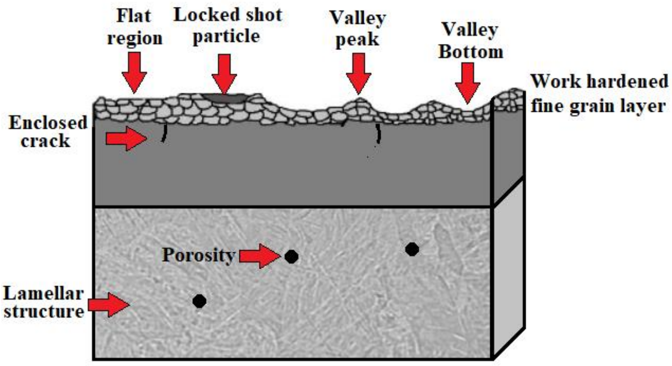

Figure 13. Schematic illustration of surface layer after shot peening treatment [97–99].

The overall favourable outcomes of shot peening process can be summed up according to [99] as:

- Grain refinement
- Increase in dislocation density
- Formation of passive layer
- Decrease in porosity
- Formation of compressive residual stresses

The According to the collection and the researches of AM DMLS manufactured samples of Ti-6Al-4V carried out by R. Żebrowski, M. Walczak and their team [20,98,100,110,111], the main advantage of shot peening is the improvement of working parameters. There is a relevant increase of hardness after that type of process from approximately 10% up to 25% for highest peening pressure of 0.4 MPa which is shown in Figure 14 [110]. In comparison to substractively manufactured Ti-6Al-4V, a similar increase was obtained for AM according to [112] from approximately 10% to 25% for higher peening pressure of 0.5 MPa which is shown in Table 5.

Preprints (www.preprints.org) | NOT PEER-REVIEWED | Posted: 18 January 2024 doi:10.20944/preprints202401.1375.v1

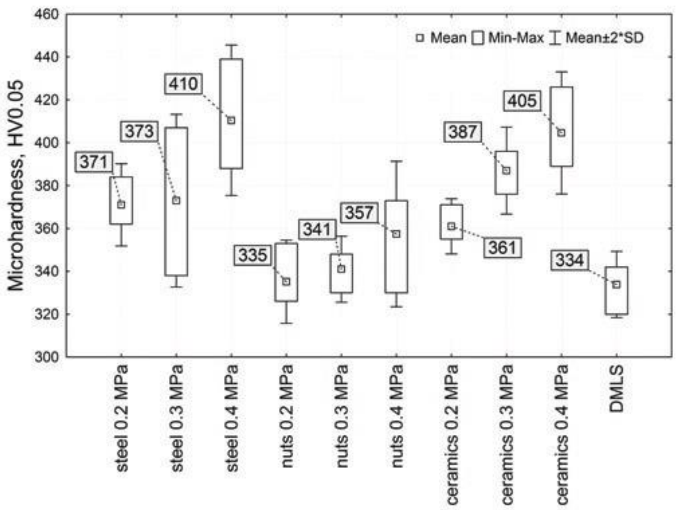

Figure 14. The hardness variation at different applied loads and shots for shot peening treatment of Ti-6Al-4V alloy [110].

Table 5. Hardness of conventionally made Ti6Al4V on top surface with different surface treatment conditions [112].

	Name of shot peening media (type of media)			
	Untreated	**SUS100 (SUS304)**	**SUS400 (SUS304)**	**FHB 80 (SiO2)**
Peening pressure	-		0.5 MPa	
Hardness	371 HV	420 HV	440 HV	470 HV

The increase of surface hardness can be explained by the fact that the creation of nanocrystalline layer after shot peening treatment on the surface of treated specimen leads to material strengthening effect [113,114].

The similar effect of increase was achieved for the group of specimens from ultimate tensile strength test as from hardness test, which means that the Ti-6Al-4V demonstrates similar correlations between hardness and UTS [98]. Results of tensile tests are shown in Figure 15

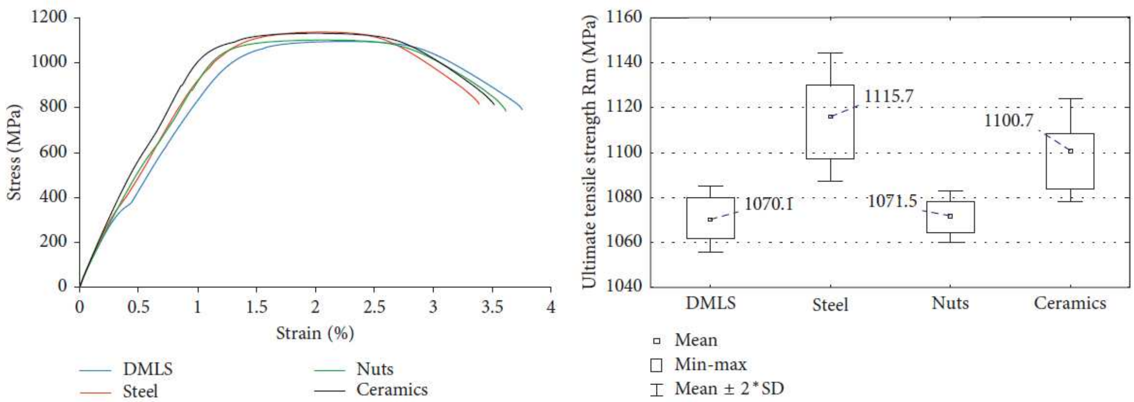

(**a**) (**b**)

Figure 15. Tensile test: (**a**) stress-strain curves of various shot peening treated specimens; (**b**) ultimate tensile strength [98].

In terms of wear and tribological performance of Ti-6Al-4V, there is decrease of surfaces friction coefficient for surfaces. There are changes associated with the use of balls which are made of Al2O3 constituting the counter-body. The comparable friction coefficient was obtained for soft surface subjection. For some surfaces, the friction coefficient increased, which is shown in Figure 16 [100]

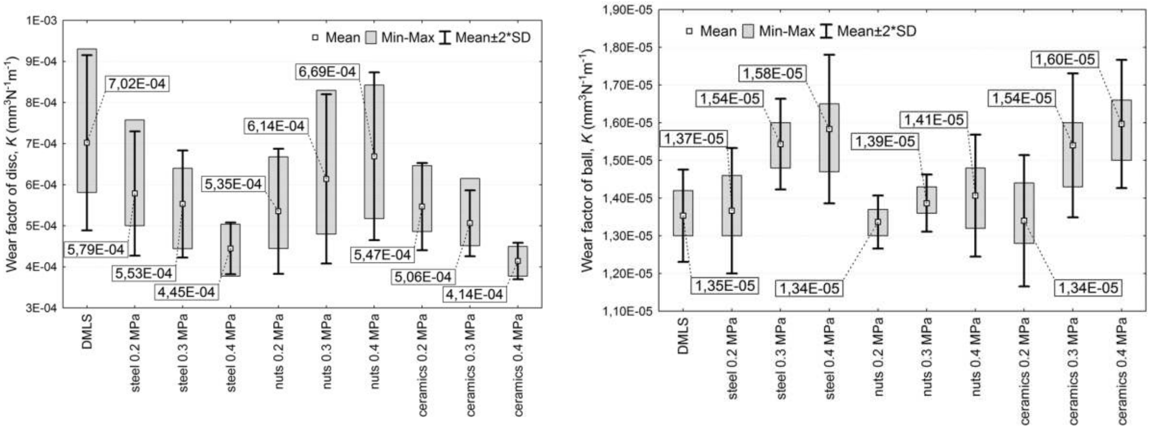

(**a**) (**b**)

Figure 16. Illustration of wear factor K for tested Ti-6Al-4V alloy: (a) surfaces; (b) counter-bodies [100].

Similar decrease of COF was obtained for substractively made Ti-6Al-4V according to [115] which is shown in Figure 17

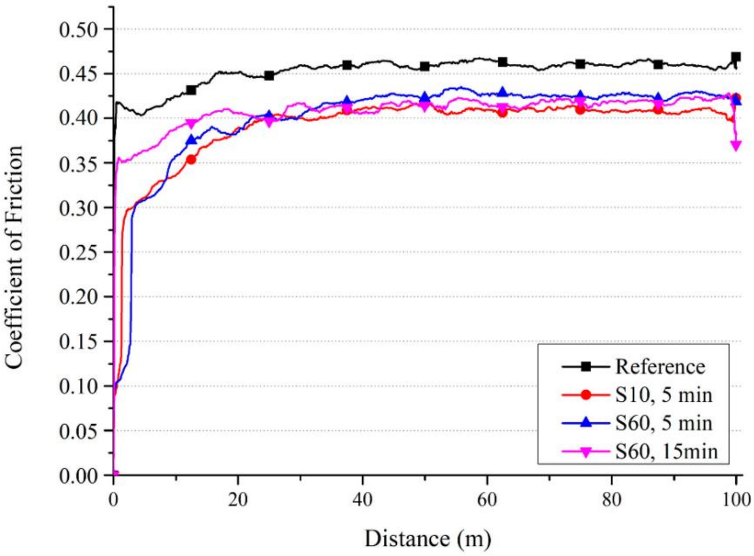

Figure 17. Characteristic of coefficient of friction to sliding distance for conventional Ti6Al4V depending on shot peening treatment [115]. Copyright MDPI, 2020.

The signs of wear of Ti-Al-4V are typical for metallic materials with significant hardness and high ductility. Prevailing wear mechanism relies on abrasion and groove forming is caused by the presence of β phase which is the cause of such an effect. The plasticity of β phase is higher than the plasticity of α phase which contributes to locally increased plastic deformation, which was confirmed by Faria et al. [116]. The wear mechanisms for AM and SM of Ti-6Al-4V after shot peening are similar as it also depends on the uniformity and quality of the surface layer which was confirmed by Airao et. al. [117]. After shot peening, the comparable structure is obtained for both AM and SM.

In terms of corrosion behaviour, there is a decrease of surfaces impedance (Figure 18), but, on the other hand, an improvement of electrochemical Ti-6Al-4V properties after shot peening process as seen in Table 6

Preprints (www.preprints.org) | NOT PEER-REVIEWED | Posted: 18 January 2024 doi:10.20944/preprints202401.1375.v1

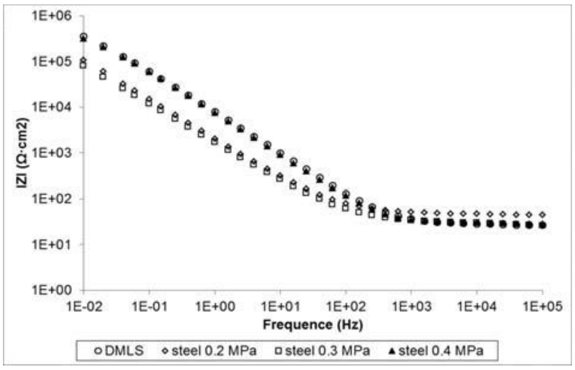

(a)

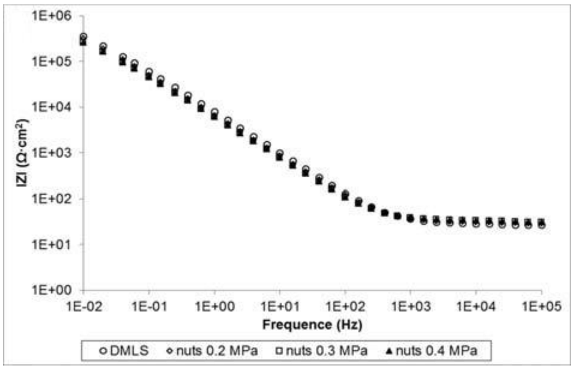

(b)

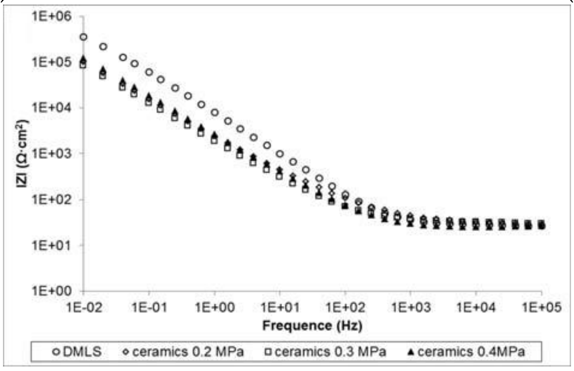

(c)

Figure 18. Bode plot characteristic of impedance module vs. frequency for surface modified: (**a**) by means of steel shot; (**b**) by means of nutshells; (**c**) by means of ceramic beads [111].

Impedance spectra shown in Figure 18 are representing the impedance module versus frequency displays close impedance values after shot peening to untreated specimens. The obtained results after shot peening are high and situated between the range of 105÷106 Ω·cm2 at low frequencies, which means that these surfaces are sufficient for bioengineering purposes with enough corrosion resistance in body fluids [113,118,119].

Table 6. Electrochemical corrosion tests in 0,9 % NaCl for various peened surfaces of Ti-6Al-4V [110].

Conditions		Current density, I_{corr} (mA/cm²)	Potential, E_{corr} (mV)	Polarization resistance R_p (kΩcm²)
Untreated		0,064	-318,6	2291
Untreated mechanically polished		0,067	-141,1	328,5
Steel CrNi	0.2 MPa	0,421	-173,5	210,5
	0.3 MPa	0,561	-207,4	138,8
	0.4 MPa	0,682	-337,1	81,2
Nuts	0.2 MPa	0,124	-106,6	346,5
	0.3 MPa	0,275	-228,5	367,4
	0.4 MPa	1,469	-279,2	349,5
Ceramic Beads	0.2 MPa	0,026	-123,8	170,8
	0.3 MPa	0,045	-151,4	206,2
	0.4 MPa	0,063	-174,3	432,8

Preprints (www.preprints.org) | NOT PEER-REVIEWED | Posted: 18 January 2024 doi:10.20944/preprints202401.1375.v1

As increase of surface hardness, the increase of corrosion resistance can be explained by the spontaneous creation of nanocrystalline layer after shot peening treatment. This passive layer created on Ti-6Al-4V surgical alloys is stable in Ringer fluid solution and is rich mainly in amorphous TiO2 [113,114]. However, more factors should be taken into account. The disorientation of the topography is reported to play a crucial role in corrosion resistance [120] as can be seen in Table 6 Mechanically polished surfaces obtained favourable electrochemical parameters. It is favourable due to low roughness values (especially of Sa parameter) and the lack of structural discontinuities in surface layer created in course of DMLS process [110]. Comparing AM to CM [121] indicates that corrosion behaviour, for polished surfaces after shot peening treatment, could be more favourable for 3D printed surfaces rather than the conventional one.

Surface roughness also influences coating adhesion such as droplet impact, wetting and solidification [122]. Another factor which has a direct impact on coating adhesion is stiffness and hardness. Comparing DMLS technology and conventional manufacturing indicates that the formation of martensitic structure during additive manufacturing like DMLS technology makes the substrate more stiff and hard of approximately 20% higher nanohardness and elastic modulus of the surface layer than the alloy fabricated by the conventional methods. This results in, for instance, a better fit between the Ecoating/Esubstrate for PVD nitride coatings which are shown in Table 7

Table 7. Mean hardness and elastic modulus of surface layer, and their ratios for DMLS and Conv. samples (Instrumented indentation test according to PN-EN ISO14577-1 standard) [20].

Substrate: Ti6Al4V	**Coating**					
	-		**AlTiN**		**TiAlN**	
	DMLS	Conv.	DMLS	Conv.	DMLS	Conv.
S_a [µm]	0,014	0,040	0,027	0,038	0,028	0,053
H_{IT}	5,7 ± 0,2	4,8 ± 0,4	25,0 ± 4,6	26,1 ± 4,3	23,6 ± 3,4	23,2 ± 3,3
E_{IT}	137,0 ± 4,1	114,5 ± 4,7	518,7 ± 129,1	559,2 ± 117,3	411,4 ± 45,8	503,5 ± 99,4
$H_{coating}/E_{coating}$	-	-	0,048	0,047	0,057	0,046
$H^3_{coating}/E^2_{coating}$	-	-	0,059	0,057	0,078	0,049
$E_{coating}/E_{substrate}$	-	-	3,79	4,88	3,00	4,40

3.3. Electropolishing

Electropolishing (EP) is a damage-free and highly efficient electrochemical surface finishing method for metal components. During electropolishing, the material works as an anode, and connects with the positive electrode of a DC power. The anode metal is oxidized into metal ions due to the loss of electrons. Then, it dissolves into the electrolyte, resulting in the removal of surface materials in order to polish, passivate and deburr the metal parts [123–127]. This method does not cause mechanical interaction, damage or leave any residual stress [128]. The schematic example of typical electropolishing setup and mechanism of electropolishing for titanium alloys are shown in Figures 19 and 20.

Preprints (www.preprints.org) | NOT PEER-REVIEWED | Posted: 18 January 2024 doi:10.20944/preprints202401.1375.v1

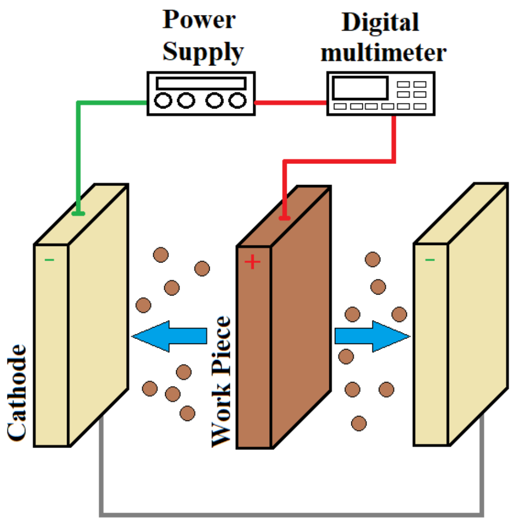

Figure 19. Schematic illustration of a typical setup of the electrolytic cell for electropolishing according to [129,130].

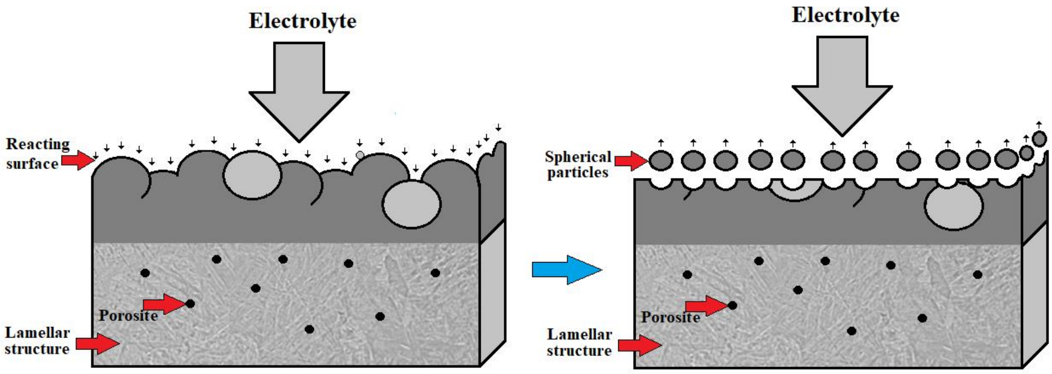

Figure 20. Mechanism of electropolishing of Ti6Al4V object after AM according to [129,131].

Electrolytes used in electrochemical processes of electropolishing titanium and titanium alloys are:

- perchloric acid-based electrolytes, such as perchloric acid/acetic acid and perchloric acid/methanol/ethylene glycol systems [132,133];
- perchloric acid-free electrolytes, for instance, methanol/sulfuric acid and ethylene glycol/NaCl [134,135];
- deep eutectic solvents (DES) such as ChCl [136,137].

Comparing mechanical polishing to electropolishing, surface layer characteristics [138] and corrosion behaviour properties [139] are more favourable for electropolishing of conventionally made Ti-6Al-4V. The literature [138–141] also indicates that surface roughness (Ra parameter) is affected by the time, current density and temperature of the process and depending on parameter selection can result in an increase (Table 9) [140] or a decrease (Table 10) [138] of roughness. Influence of temperature on material roughness after electropolishing treatment is shown in Table 8.

Preprints (www.preprints.org) | NOT PEER-REVIEWED | Posted: 18 January 2024 doi:10.20944/preprints202401.1375.v1

Table 8. Surface roughness parameters (Ra) and empty pits diameters of Ti-6Al-4V titanium alloy electrochemically etched in Ethaline at different current densities (t = 25°C, T = 20 min). According to [140].

Conditions	Current density of treatment ($mA{\cdot}cm^{-2}$)	Ra (nm)	Pit diameter (μm)
Untreated	-	321	-
Electrochemically etched	5	651	25
	10	967	24
	15	504	27

Table 9. Comparison of roughness for mechanical and electropolishing treatment [138].

Roughness	Microstructure at various cooling medium					
	Untreated	Electropolishing 100s	Electropolishing 200s	Electropolishing 300s	Mechanical #1000SiC	Mechanical #1500SiC
Micro [nm]	120,05 ± 7,89	58,72 ± 3,68	12,63 ± 0,81	10,33 ± 1,14	98,30 ± 3,79	86,42 ± 2,05
Macro [μm]	2,34 ± 0,07	1,68 ± 0,02	0,75 ± 0,05	0,68 ± 0,03	2,04 ± 0,03	1,82 ± 0,09

Table 10. Temperature impact on Ti6Al4V specimens roughness during electropolishing (current density = 0,19 A·cm-2, T = 8 min) according to [141].

Temperature	Roughness		
	R_a (nm)	R_{ms} (nm)	R_z (nm)
7°C	7,4	10,0	39,7
18°C	6,1	8,1	27,5
25°C	6,4	8,1	26,6

Although many previous investigations have reported the properties and electrochemical behaviours of traditional titanium alloys after electropolishing based on different bath components and process parameters, the special surface state of additively manufactured titanium alloys has limited their usage [142]. This can be ascribed to the reason that the titanium alloys fabricated by AM often have incomplete melting powder, which generates an oxide film-like ceramic with high hardness and low chemical activity [143].

According to Zhang research [131] on electropolishing of additively manufactured Ti-6Al-4V specimens by selective laser melting, optimal electrochemical treatment is able to improve roughness (Table 11) and impedance (Table 12) of the titanium alloy.

Table 11. Surface roughness, weight loss and impedance parameters after different EP times for Ti-6Al-4V alloy according to [131].

Sample No.	0	1	2	3	4
Polishing time (min.)	untreated	5	10	15	20
Weight loss [%]	-	5,98	10,82	14,76	16,29
R_a [μm]	6,33	2,01	1,63	1,132	1,72
R_L ($\Omega{\cdot}cm^2$)	-	20,69	16,44	21,49	23,29
Q_c ($F{\cdot}cm^{-2}$)	-	2,016e-2	2,507e-5	5,625e-5	4,656e-5
R_c ($\Omega{\cdot}cm^2$)	-	758,40	8,56	12,72	23,26
Q_d ($F{\cdot}cm^{-2}$)	-	-	2,663e-6	3,724e-6	2,051e-6

Preprints (www.preprints.org) | NOT PEER-REVIEWED | Posted: 18 January 2024 doi:10.20944/preprints202401.1375.v1

R_t (Ω·cm²)	-	-	-7,152e5	1,014e6	5,128e5
Chi-squared (X^2)	-	2,02e-3	1,48e-3	7,97e-4	1,59e-3

4. Properties of Ti6Al4V Manufactured Using Conventional Methods and Additive Manufacturing Methods

Many fields of application could benefit from the properties provided by shot peening process but they are overshadowed by the unfavourable characteristics from the roughened surface. The example of this is the automotive branch where reports suggests that the contact fatigue resistance of shot peened austempered ductile iron gears has poor performance due to the roughness of the surface layer [144]. Another issue which challenges its successful application in some fields is the potential presence of locked shot fragments on the treated surfaces introducing potential crack nucleation sites (Figure 21). In biomedical applications, these particles could be responsible for early implant failure [145].

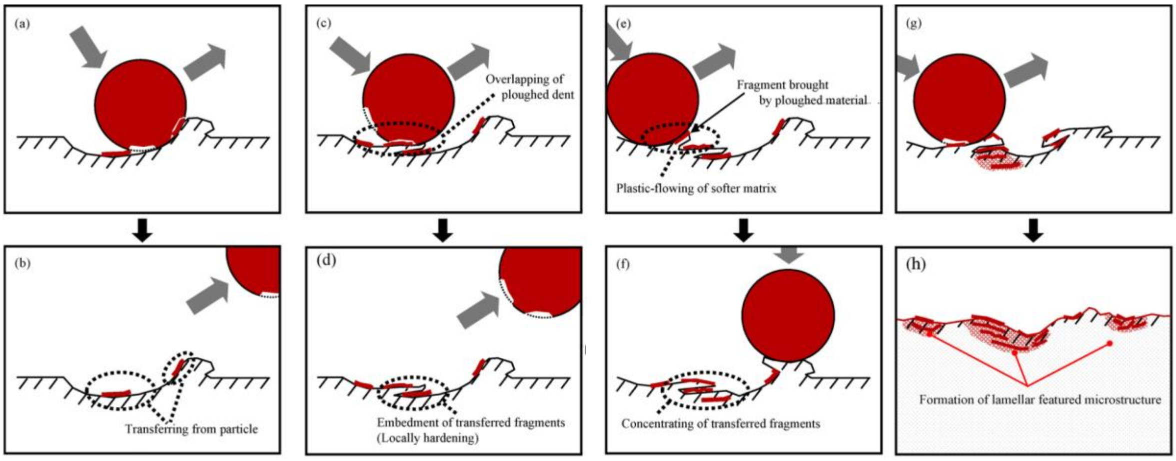

Figure 21. Embedment of shot particle in material surface layer according to [114]. Copyright Elsevier, 2009.

The topography of the surface treated Ti-6Al-4V alloy modified by shot grains penetrates into surface layer. The effect of this process is visible in Figure 22. Penetrating shot is located in structural discontinuities or directly on the surface as a result of its high kinetic energy because the properties of material being printed contribute to formation of these lamellar structures [111].

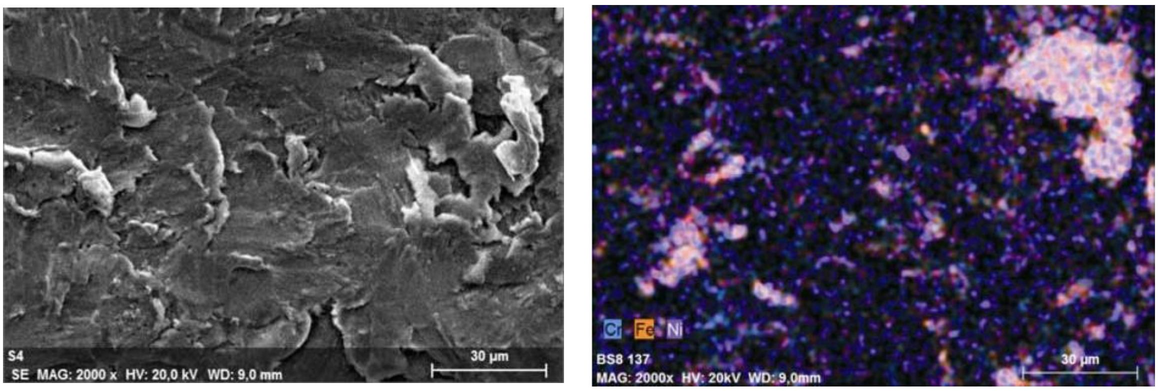

(a) (b)

Figure 22. Formation of lamellar featured microstructure on Ti6Al4V surface after SP with CrNi shots (**a**) shot inclusions on specimens surface; (**b**) mapping of elements originating from steel shot [111].

In this regard, it is necessary to control the peening processes to remove embedded remains of peening media in order to meet the requirements of smooth and defects-free surface for certain applications. This suggested method could provide further improvement of material properties such as wear and corrosion resistance [146].

Some research was done by M. Kiel; J. Szewczenko's team et. al. [147–150] of combining shot peening and electropolishing for conventionally made Ti-6Al-4V which show promising result. The effect of combining shot peening and electrolytical polishing on corrosion resistance is shown in Table 12

Table 12. Corrosion behaviour after different surface treatment of Ti-6Al-4V ELI alloy [150].

Surface treatment processes	E_{corr} [mV]	I_{corr} [μA·cm^{-2}]	R_p [kΩ·cm^2]
Shot peening, sandblasting	-266	0,047	551
Shot peening, electropolishing	-95	0,053	489
Shot peening, mechanical polishing, electropolishing	-172	0,069	377,15

5. Summary

This paper reviews the basic information regarding shot peening methods and the effects of the shot peening (SP) and electropolishing (EP) treatments on the surface layer properties of Ti6Al4V components and compares its effects depending on manufacturing process (AM or CM). In addition, the literature survey done regarding the shot peening and electropolishing treatments allows one to indicate the research gaps and further directions of the surface treatment process of the titanium alloys.

There is a research gap since, as far as the authors' knowledge goes, there are no studies describing a hybrid treatment consisting of a combination of shot peening and electropolishing methods on additively manufactured objects including Ti6Al4V titanium alloy.

A research area in this direction could include, for instance, the application of EP treatment after SP, or EP treatment followed by SP. In addition, the optimisation of hybrid process parameters such as different peening times, intensities or shot sizes in the SP process and different polishing times, the type of electrolytes and voltage in the EP process are also required.

Although many previous investigations have reported the properties and electrochemical behaviours of traditional titanium alloys after electropolishing based on different bath components and process parameters, the special surface state of additively manufactured titanium alloys signifies the need for further investigations on that matter.

Metal parts fabricated directly by AM technology, even though they seem as a good quality product after the manufacturing process, are usually not ready for the service in their as-built state. For about 60-70% 3D-printed objects, additional processes of surface modifying treatment are needed as a result of surface defects and discontinuities in their surface layer.

The results obtained by the peening of additive technologies may differ depending on the method used for printing and the parameters or gas used in the shot peening process and employed peening method. Increasing the intensity and parameters of the peening process does not always lead to positive results as roughness and structural integrity can suffer in particular.

Few reports suggest that electropolishing reduces the presence of embedded fragments after shot peening treatment and smooths the surface of peened samples, which could be beneficial for properties of titanium alloys.

The literature gap leading to the scope of future work seems to be in need of the investigation of the effects of shot peening and combined peening and electropolishing on the anti-wear and corrosion performance of additively manufactured titanium alloys.

Author Contributions: Conceptualization, W.O., M.W. and M.S.; methodology, W.O.; software, W.O.; validation, M.S., M.W. and W.O.; formal analysis, W.O.; investigation, W.O ; resources, W.O.; data curation, W.O; writing—original draft preparation, W.O.; writing—review and editing, M.W., M.S. and W.O. ; visualisation, W.O.; supervision, M.W and M.S.; project administration, M.W.; funding acquisition, M.W. and M.S.; All authors have read and agreed to the published version of the manuscript.

Funding: The APC publication fee was fully covered by the authors' vouchers.

Institutional Review Board Statement: Not applicable.

Informed Consent Statement: Not applicable.

Data Availability Statement: No new data were created or analyzed in this study. Data sharing is not applicable to this article.

Conflicts of Interest: The authors declare no conflict of interest.

References

1. Cui, C.; Hu, B.; Zhao, L.; Liu, S. Titanium Alloy Production Technology, Market Prospects and Industry Development. *Materials & Design* **2011**, *32*, 1684–1691, doi:10.1016/j.matdes.2010.09.011.
2. Liu, S.; Shin, Y.C. Additive Manufacturing of Ti6Al4V Alloy: A Review. *Materials & Design* **2019**, *164*, 107552, doi:10.1016/j.matdes.2018.107552.
3. Pushp, P.; Dasharath, S.M.; Arati, C. Classification and Applications of Titanium and Its Alloys. *Materials Today: Proceedings* **2022**, *54*, 537–542, doi:10.1016/j.matpr.2022.01.008.
4. Sonntag, R.; Reinders, J.; Gibmeier, J.; Kretzer, J.P. Fatigue Strengthening of an Orthopedic Ti6Al4V Alloy: What Is the Potential of a Final Shot Peening Process? In *Biomaterials and Medical Tribology*; Elsevier, 2013; pp. 217–237 ISBN 978-0-85709-017-1.
5. Cook, S.; Barrack, R.; Clemow, A. Corrosion and Wear at the Modular Interface of Uncemented Femoral Stems. *The Journal of Bone and Joint Surgery. British volume* **1994**, *76-B*, 68–72, doi:10.1302/0301-620X.76B1.8300685.
6. Kretzer, J.P.; Jakubowitz, E.; Krachler, M.; Thomsen, M.; Heisel, C. Metal Release and Corrosion Effects of Modular Neck Total Hip Arthroplasty. *International Orthopaedics (SICOT)* **2009**, *33*, 1531–1536, doi:10.1007/s00264-009-0729-x.
7. Huang, H.; Lan, P.-H.; Zhang, Y.-Q.; Li, X.-K.; Zhang, X.; Yuan, C.-F.; Zheng, X.-B.; Guo, Z. Surface Characterization and in Vivo Performance of Plasma-Sprayed Hydroxyapatite-Coated Porous Ti6Al4V Implants Generated by Electron Beam Melting. *Surface and Coatings Technology* **2015**, *283*, 80–88, doi:10.1016/j.surfcoat.2015.10.047.
8. Čapek, J.; Machová, M.; Fousová, M.; Kubásek, J.; Vojtěch, D.; Fojt, J.; Jablonská, E.; Lipov, J.; Ruml, T. Highly Porous, Low Elastic Modulus 316L Stainless Steel Scaffold Prepared by Selective Laser Melting. *Materials Science and Engineering: C* **2016**, *69*, 631–639, doi:10.1016/j.msec.2016.07.027.
9. Long, M.; Rack, H.J. Titanium Alloys in Total Joint Replacement—a Materials Science Perspective. *Biomaterials* **1998**, *19*, 1621–1639, doi:10.1016/S0142-9612(97)00146-4.
10. Miranda, G.; Araújo, A.; Bartolomeu, F.; Buciumeanu, M.; Carvalho, O.; Souza, J.C.M.; Silva, F.S.; Henriques, B. Design of Ti6Al4V-HA Composites Produced by Hot Pressing for Biomedical Applications. *Materials & Design* **2016**, *108*, 488–493, doi:10.1016/j.matdes.2016.07.023.
11. Ma, X.; Chen, Z.; Zhong, D.; Luo, S.N.; Xiao, L.; Lu, W.; Zhang, S. Effect of Rotationally Accelerated Shot Peening on the Microstructure and Mechanical Behavior of a Metastable β Titanium Alloy. *Journal of Materials Science & Technology* **2021**, *75*, 27–38, doi:10.1016/j.jmst.2020.10.034.
12. Benedetti, M.; Torresani, E.; Leoni, M.; Fontanari, V.; Bandini, M.; Pederzolli, C.; Potrich, C. The Effect of Post-Sintering Treatments on the Fatigue and Biological Behavior of Ti-6Al-4V ELI Parts Made by Selective Laser Melting. *Journal of the Mechanical Behavior of Biomedical Materials* **2017**, *71*, 295–306, doi:10.1016/j.jmbbm.2017.03.024.
13. Rautio, T.; Jaskari, M.; Järvenpää, A. Surface Roughness Improvement of Pbf-Lb Manufactured 316l with Dry Electropolishing. *KEM* **2023**, *972*, 3–12, doi:10.4028/p-SaeI5W.
14. Kim, K.M.; Shim, H.-S.; Seo, M.J.; Hur, D.H. Corrosion Control of Alloy 690 by Shot Peening and Electropolishing under Simulated Primary Water Condition of PWRs. *Advances in Materials Science and Engineering* **2015**, *2015*, 1–9, doi:10.1155/2015/357624.
15. Lan, L.; Xin, R.; Jin, X.; Gao, S.; He, B.; Rong, Y.; Min, N. Effects of Laser Shock Peening on Microstructure and Properties of Ti–6Al–4V Titanium Alloy Fabricated via Selective Laser Melting. *Materials* **2020**, *13*, 3261, doi:10.3390/ma13153261.
16. Chen, S.; Zhang, Y.; Wu, Q.; Gao, H.; Gao, Z.; Li, X. Effect of Solid-State Phase Transformation on Residual Stress of Selective Laser Melting Ti6Al4V. *Materials Science and Engineering: A* **2021**, *819*, 141299, doi:10.1016/j.msea.2021.141299.

17. Mahmud, A.; Huynh, T.; Zhou, L.; Hyer, H.; Mehta, A.; Imholte, D.D.; Woolstenhulme, N.E.; Wachs, D.M.; Sohn, Y. Mechanical Behavior Assessment of Ti-6Al-4V ELI Alloy Produced by Laser Powder Bed Fusion. *Metals* **2021**, *11*, 1671, doi:10.3390/met11111671.
18. Motyka, M.; Baran-Sadleja, A.; Sieniawski, J.; Wierzbinska, M.; Gancarczyk, K. Decomposition of Deformed α ′(α ″) Martensitic Phase in Ti–6Al–4V Alloy. *Materials Science and Technology* **2019**, *35*, 260–272, doi:10.1080/02670836.2018.1466418.
19. Dasgupta, S.; Singh, Y.P. Additive Manufacturing Techniques Used for Preparation of Scaffolds in Bone Repair and Regeneration. In *Advances in Additive Manufacturing Artificial Intelligence, Nature-Inspired, and Biomanufacturing*; Elsevier, 2023; pp. 103–127 ISBN 978-0-323-91834-3.
20. Walczak, M.; Pasierbiewicz, K.; Szala, M. Effect of Ti6Al4V Substrate Manufacturing Technology on the Properties of PVD Nitride Coatings. *Acta Phys. Pol. A* **2022**, *142*, 723–732, doi:10.12693/APhysPolA.142.723.
21. Ahmed, T.; Rack, H.J. Phase Transformations during Cooling in A+β Titanium Alloys. *Materials Science and Engineering: A* **1998**, *243*, 206–211, doi:10.1016/S0921-5093(97)00802-2.
22. Omoniyi, P.O.; Akinlabi, E.T.; Mahamood, R.M. Heat Treatments of Ti6Al4V Alloys for Industrial Applications: An Overview. *IOP Conf. Ser.: Mater. Sci. Eng.* **2021**, *1107*, 012094, doi:10.1088/1757-899X/1107/1/012094.
23. Fidan, S.; Avcu, E.; Karakulak, E.; Yamanoglu, R.; Zeren, M.; Sinmazcelik, T. Effect of Heat Treatment on Erosive Wear Behaviour of Ti6Al4V Alloy. *Materials Science and Technology* **2013**, *29*, 1088–1094, doi:10.1179/1743284713Y.0000000239.
24. Rajan Soundararajan, S.; Vishnu, J.; Manivasagam, G.; Rao Muktinutalapati, N. Processing of Beta Titanium Alloys for Aerospace and Biomedical Applications. In *Titanium Alloys - Novel Aspects of Their Processing [Working Title]*; IntechOpen, 2018.
25. Vrancken, B.; Thijs, L.; Kruth, J.-P.; Van Humbeeck, J. Heat Treatment of Ti6Al4V Produced by Selective Laser Melting: Microstructure and Mechanical Properties. *Journal of Alloys and Compounds* **2012**, *541*, 177–185, doi:10.1016/j.jallcom.2012.07.022.
26. Venkatesh, B.D.; Chen, D.L.; Bhole, S.D. Effect of Heat Treatment on Mechanical Properties of Ti–6Al–4V ELI Alloy. *Materials Science and Engineering: A* **2009**, *506*, 117–124, doi:10.1016/j.msea.2008.11.018.
27. Zhai, Y.; Galarraga, H.; Lados, D.A. Microstructure, Static Properties, and Fatigue Crack Growth Mechanisms in Ti-6Al-4V Fabricated by Additive Manufacturing: LENS and EBM. *Engineering Failure Analysis* **2016**, *69*, 3–14, doi:10.1016/j.engfailanal.2016.05.036.
28. Koike, M.; Greer, P.; Owen, K.; Lilly, G.; Murr, L.E.; Gaytan, S.M.; Martinez, E.; Okabe, T. Evaluation of Titanium Alloys Fabricated Using Rapid Prototyping Technologies—Electron Beam Melting and Laser Beam Melting. *Materials* **2011**, *4*, 1776–1792, doi:10.3390/ma4101776.
29. Vilaro, T.; Colin, C.; Bartout, J.D. As-Fabricated and Heat-Treated Microstructures of the Ti-6Al-4V Alloy Processed by Selective Laser Melting. *Metall Mater Trans A* **2011**, *42*, 3190–3199, doi:10.1007/s11661-011-0731-y.
30. Zhu, Y.; Zou, J.; Yang, H. Wear Performance of Metal Parts Fabricated by Selective Laser Melting: A Literature Review. *J. Zhejiang Univ. Sci. A* **2018**, *19*, 95–110, doi:10.1631/jzus.A1700328.
31. Kranz, J.; Herzog, D.; Emmelmann, C. Design Guidelines for Laser Additive Manufacturing of Lightweight Structures in TiAl6V4. *Journal of Laser Applications* **2015**, *27*, S14001, doi:10.2351/1.4885235.
32. Singla, A.K.; Banerjee, M.; Sharma, A.; Singh, J.; Bansal, A.; Gupta, M.K.; Khanna, N.; Shahi, A.S.; Goyal, D.K. Selective Laser Melting of Ti6Al4V Alloy: Process Parameters, Defects and Post-Treatments. *Journal of Manufacturing Processes* **2021**, *64*, 161–187, doi:10.1016/j.jmapro.2021.01.009.
33. Sun, S.; Zhang, D.; Palanisamy, S.; Liu, Q.; Dargusch, M.S. Mechanical Properties and Deformation Mechanisms of Martensitic Ti6Al4V Alloy Processed by Laser Powder Bed Fusion and Water Quenching. *Materials Science and Engineering: A* **2022**, *839*, 142817, doi:10.1016/j.msea.2022.142817.
34. Lv, C.; Wang, J.; Li, H.; Yin, Q.; Liu, W.; Shen, S. Dynamics of the Laser–Powder Interaction in the Ti6Al4V Powder Feeding Process of Laser-Directed Energy Deposition Additive Manufacturing. *Journal of Materials Research and Technology* **2023**, *27*, 6376–6385, doi:10.1016/j.jmrt.2023.11.099.
35. Shen, B.; Li, H.; Liu, S.; Zou, J.; Shen, S.; Wang, Y.; Zhang, T.; Zhang, D.; Chen, Y.; Qi, H. Influence of Laser Post-Processing on Pore Evolution of Ti–6Al–4V Alloy by Laser Powder Bed Fusion. *Journal of Alloys and Compounds* **2020**, *818*, 152845, doi:10.1016/j.jallcom.2019.152845.
36. Cao, F.; Zhang, T.; Ryder, M.A.; Lados, D.A. A Review of the Fatigue Properties of Additively Manufactured Ti-6Al-4V. *JOM* **2018**, *70*, 349–357, doi:10.1007/s11837-017-2728-5.
37. Harun, W.S.W.; Kamariah, M.S.I.N.; Muhamad, N.; Ghani, S.A.C.; Ahmad, F.; Mohamed, Z. A Review of Powder Additive Manufacturing Processes for Metallic Biomaterials. *Powder Technology* **2018**, *327*, 128–151, doi:10.1016/j.powtec.2017.12.058.
38. Alcisto, J.; Enriquez, A.; Garcia, H.; Hinkson, S.; Steelman, T.; Silverman, E.; Valdovino, P.; Gigerenzer, H.; Foyos, J.; Ogren, J.; et al. Tensile Properties and Microstructures of Laser-Formed Ti-6Al-4V. *J. of Materi Eng and Perform* **2011**, *20*, 203–212, doi:10.1007/s11665-010-9670-9.

39. Seifi, M.; Salem, A.; Beuth, J.; Harrysson, O.; Lewandowski, J.J. Overview of Materials Qualification Needs for Metal Additive Manufacturing. *JOM* **2016**, *68*, 747–764, doi:10.1007/s11837-015-1810-0.
40. Simonelli, M.; Tse, Y.Y.; Tuck, C. Effect of the Build Orientation on the Mechanical Properties and Fracture Modes of SLM Ti–6Al–4V. *Materials Science and Engineering: A* **2014**, *616*, 1–11, doi:10.1016/j.msea.2014.07.086.
41. Bhandari, L.; Gaur, V. On Study of Process Induced Defects-Based Fatigue Performance of Additively Manufactured Ti6Al4V Alloy. *Additive Manufacturing* **2022**, *60*, 103227, doi:10.1016/j.addma.2022.103227.
42. Wysocki, B.; Maj, P.; Sitek, R.; Buhagiar, J.; Kurzydłowski, K.; Święszkowski, W. Laser and Electron Beam Additive Manufacturing Methods of Fabricating Titanium Bone Implants. *Applied Sciences* **2017**, *7*, 657, doi:10.3390/app7070657.
43. Guo, S.; Li, Y.; Gu, J.; Liu, J.; Peng, Y.; Wang, P.; Zhou, Q.; Wang, K. Microstructure and Mechanical Properties of Ti6Al4V/ B4C Titanium Matrix Composite Fabricated by Selective Laser Melting (SLM). *Journal of Materials Research and Technology* **2023**, *23*, 1934–1946, doi:10.1016/j.jmrt.2023.01.126.
44. Facchini, L.; Magalini, E.; Robotti, P.; Molinari, A.; Höges, S.; Wissenbach, K. Ductility of a Ti-6Al-4V Alloy Produced by Selective Laser Melting of Prealloyed Powders. *Rapid Prototyping Journal* **2010**, *16*, 450–459, doi:10.1108/13552541011083371.
45. Bordin, A.; Bruschi, S.; Ghiotti, A.; Bucciotti, F.; Facchini, L. Comparison between Wrought and EBM Ti6Al4V Machinability Characteristics. *KEM* **2014**, *611–612*, 1186–1193, doi:10.4028/www.scientific.net/KEM.611-612.1186.
46. Ishfaq, K.; Abdullah, M.; Mahmood, M.A. A State-of-the-Art Direct Metal Laser Sintering of Ti6Al4V and AlSi10Mg Alloys: Surface Roughness, Tensile Strength, Fatigue Strength and Microstructure. *Optics & Laser Technology* **2021**, *143*, 107366, doi:10.1016/j.optlastec.2021.107366.
47. Karolewska, K.; Ligaj, B.; Boroński, D. Strain Analysis of Ti6Al4V Titanium Alloy Samples Using Digital Image Correlation. *Materials* **2020**, *13*, 3398, doi:10.3390/ma13153398.
48. Guzanová, A.; Ižaríková, G.; Brezinová, J.; Živčák, J.; Draganovská, D.; Hudák, R. Influence of Build Orientation, Heat Treatment, and Laser Power on the Hardness of Ti6Al4V Manufactured Using the DMLS Process. *Metals* **2017**, *7*, 318, doi:10.3390/met7080318.
49. Sharma, M.; Soni, M. Direct Metal Laser Sintering of TI6Al4V Alloy for Patient-Specific Temporo Mandibular Joint Prosthesis and Implant. *Materials Today: Proceedings* **2021**, *38*, 333–339, doi:10.1016/j.matpr.2020.07.417.
50. Mierzejewska, Ż.A. Effect of Laser Energy Density, Internal Porosity and Heat Treatment on Mechanical Behavior of Biomedical Ti6Al4V Alloy Obtained with DMLS Technology. *Materials* **2019**, *12*, 2331, doi:10.3390/ma12142331.
51. Thijs, L.; Verhaeghe, F.; Craeghs, T.; Humbeeck, J.V.; Kruth, J.-P. A Study of the Microstructural Evolution during Selective Laser Melting of Ti–6Al–4V. *Acta Materialia* **2010**, *58*, 3303–3312, doi:10.1016/j.actamat.2010.02.004.
52. Motyka, M. Martensite Formation and Decomposition during Traditional and AM Processing of Two-Phase Titanium Alloys—An Overview. *Metals* **2021**, *11*, 481, doi:10.3390/met11030481.
53. Bartolomeu, F.; Gasik, M.; Silva, F.S.; Miranda, G. Mechanical Properties of Ti6Al4V Fabricated by Laser Powder Bed Fusion: A Review Focused on the Processing and Microstructural Parameters Influence on the Final Properties. *Metals* **2022**, *12*, 986, doi:10.3390/met12060986.
54. Vrancken, B.; Buls, S.; Kruth, J.; Humbeeck, J.V. Preheating of Selective Laser Melted Ti6Al4V: Microstructure and Mechanical Properties. In *Proceedings of the 13th World Conference on Titanium*; Venkatesh, V., Pilchak, A.L., Allison, J.E., Ankem, S., Boyer, R., Christodoulou, J., Fraser, H.L., Imam, M.A., Kosaka, Y., Rack, H.J., Chatterjee, A., Woodfield, A., Eds.; Wiley, 2016; pp. 1269–1277 ISBN 978-1-119-28326-3.
55. Kogo, B.; Xu, C.; Wang, B.; Chizari, M.; Reza Kashyzadeh, K.; Ghorbani, S. An Experimental Analysis to Determine the Load-Bearing Capacity of 3D Printed Metals. *Materials* **2022**, *15*, 4333, doi:10.3390/ma15124333.
56. Kim, F.H.; Moylan, S.P. *Literature Review of Metal Additive Manufacturing Defects*; National Institute of Standards and Technology: Gaithersburg, MD, 2018; p. NIST AMS 100-16;
57. Polozov, I.; Gracheva, A.; Popovich, A. Interface Characterization of Bimetallic Ti-6Al-4V/Ti2AlNb Structures Prepared by Selective Laser Melting. *Materials* **2022**, *15*, 8528, doi:10.3390/ma15238528.
58. Gaur, V.; Doquet, V.; Persent, E.; Mareau, C.; Roguet, E.; Kittel, J. Surface versus Internal Fatigue Crack Initiation in Steel: Influence of Mean Stress. *International Journal of Fatigue* **2016**, *82*, 437–448, doi:10.1016/j.ijfatigue.2015.08.028.
59. Keshavarzkermani, A.; Sadowski, M.; Ladani, L. Direct Metal Laser Melting of Inconel 718: Process Impact on Grain Formation and Orientation. *Journal of Alloys and Compounds* **2018**, *736*, 297–305, doi:10.1016/j.jallcom.2017.11.130.

60. Zhang, Y.; Zhang, J. Finite Element Simulation and Experimental Validation of Distortion and Cracking Failure Phenomena in Direct Metal Laser Sintering Fabricated Component. *Additive Manufacturing* **2017**, *16*, 49–57, doi:10.1016/j.addma.2017.05.002.
61. Zhao, X.; Iyer, A.; Promoppatum, P.; Yao, S.-C. Numerical Modeling of the Thermal Behavior and Residual Stress in the Direct Metal Laser Sintering Process of Titanium Alloy Products. *Additive Manufacturing* **2017**, *14*, 126–136, doi:10.1016/j.addma.2016.10.005.
62. Anand, M.; Das, A.K. Issues in Fabrication of 3D Components through DMLS Technique: A Review. *Optics & Laser Technology* **2021**, *139*, 106914, doi:10.1016/j.optlastec.2021.106914.
63. Martinho, P.G. Rapid Manufacturing and Tooling. In *Design and Manufacturing of Plastics Products*; Elsevier, 2021; pp. 381–456 ISBN 978-0-12-819775-2.
64. Hussain, M.; Mandal, V.; Kumar, V.; Das, A.K.; Ghosh, S.K. Development of TiN Particulates Reinforced SS316 Based Metal Matrix Composite by Direct Metal Laser Sintering Technique and Its Characterization. *Optics & Laser Technology* **2017**, *97*, 46–59, doi:10.1016/j.optlastec.2017.06.006.
65. Zhou, M.; Deng, X. Melting and Resolidification of Direct Metal Laser Sintering with Multiscale Nonequilibrium Model. *Journal of Thermophysics and Heat Transfer* **2019**, *33*, 78–86, doi:10.2514/1.T5449.
66. Mierzejewska, Ż.A.; Hudák, R.; Sidun, J. Mechanical Properties and Microstructure of DMLS Ti6Al4V Alloy Dedicated to Biomedical Applications. *Materials* **2019**, *12*, 176, doi:10.3390/ma12010176.
67. Tebianian, M.; Aghaie, S.; Razavi Jafari, N.; Elmi Hosseini, S.; Pereira, A.; Fernandes, F.; Farbakhti, M.; Chen, C.; Huo, Y. A Review of the Metal Additive Manufacturing Processes. *Materials* **2023**, *16*, 7514, doi:10.3390/ma16247514.
68. Isik, M.; Yildiz, M.; Secer, R.O.; Sen, C.; Bilgin, G.M.; Orhangul, A.; Akbulut, G.; Javidrad, H.; Koc, B. Fabrication of Electron Beam Melted Titanium Aluminide: The Effects of Machining Parameters and Heat Treatment on Surface Roughness and Hardness. *Metals* **2023**, *13*, 1952, doi:10.3390/met13121952.
69. Tan, X.; Kok, Y.; Tor, S.B.; Chua, C.K. Application of Electron Beam Melting (EBM) in Additive Manufacturing of an Impeller. In Proceedings of the Proceedings of the 1st International Conference on Progress in Additive Manufacturing; Research Publishing Services, 2014; pp. 327–332.
70. Cho, K.; Kawabata, H.; Hayashi, T.; Yasuda, H.Y.; Nakashima, H.; Takeyama, M.; Nakano, T. Peculiar Microstructural Evolution and Tensile Properties of β-Containing γ-TiAl Alloys Fabricated by Electron Beam Melting. *Additive Manufacturing* **2021**, *46*, 102091, doi:10.1016/j.addma.2021.102091.
71. Bansal, S.A.; Khanna, V.; Gupta, P. *Metal Matrix Composites: Fabrication, Production, and 3D Printing (Vol. 1)*; 1st ed.; CRC Press: Boca Raton, 2022; ISBN 978-1-00-319489-7.
72. Trevisan, F.; Calignano, F.; Aversa, A.; Marchese, G.; Lombardi, M.; Biamino, S.; Ugues, D.; Manfredi, D. Additive Manufacturing of Titanium Alloys in the Biomedical Field: Processes, Properties and Applications. *Journal of Applied Biomaterials & Functional Materials* **2018**, *16*, 57–67, doi:10.5301/jabfm.5000371.
73. Sanaei, N.; Fatemi, A. Defects in Additive Manufactured Metals and Their Effect on Fatigue Performance: A State-of-the-Art Review. *Progress in Materials Science* **2021**, *117*, 100724, doi:10.1016/j.pmatsci.2020.100724.
74. Ng, G.K.L.; Jarfors, A.E.W.; Bi, G.; Zheng, H.Y. Porosity Formation and Gas Bubble Retention in Laser Metal Deposition. *Appl. Phys. A* **2009**, *97*, 641–649, doi:10.1007/s00339-009-5266-3.
75. Hrabe, N.; Quinn, T. Effects of Processing on Microstructure and Mechanical Properties of a Titanium Alloy (Ti–6Al–4V) Fabricated Using Electron Beam Melting (EBM), Part 1: Distance from Build Plate and Part Size. *Materials Science and Engineering: A* **2013**, *573*, 264–270, doi:10.1016/j.msea.2013.02.064.
76. Cunningham, R.; Narra, S.P.; Montgomery, C.; Beuth, J.; Rollett, A.D. Synchrotron-Based X-Ray Microtomography Characterization of the Effect of Processing Variables on Porosity Formation in Laser Power-Bed Additive Manufacturing of Ti-6Al-4V. *JOM* **2017**, *69*, 479–484, doi:10.1007/s11837-016-2234-1.
77. Hojjatzadeh, S.M.H.; Parab, N.D.; Guo, Q.; Qu, M.; Xiong, L.; Zhao, C.; Escano, L.I.; Fezzaa, K.; Everhart, W.; Sun, T.; et al. Direct Observation of Pore Formation Mechanisms during LPBF Additive Manufacturing Process and High Energy Density Laser Welding. *International Journal of Machine Tools and Manufacture* **2020**, *153*, 103555, doi:10.1016/j.ijmachtools.2020.103555.
78. Hrabe, N.; Gnäupel-Herold, T.; Quinn, T. Fatigue Properties of a Titanium Alloy (Ti–6Al–4V) Fabricated via Electron Beam Melting (EBM): Effects of Internal Defects and Residual Stress. *International Journal of Fatigue* **2017**, *94*, 202–210, doi:10.1016/j.ijfatigue.2016.04.022.
79. Sandell, V.; Hansson, T.; Roychowdhury, S.; Månsson, T.; Delin, M.; Åkerfeldt, P.; Antti, M.-L. Defects in Electron Beam Melted Ti-6Al-4V: Fatigue Life Prediction Using Experimental Data and Extreme Value Statistics. *Materials* **2021**, *14*, 640, doi:10.3390/ma14030640.
80. Hassan, M.S.; Zaman, S.; Dantzler, J.Z.R.; Leyva, D.H.; Mahmud, M.S.; Ramirez, J.M.; Gomez, S.G.; Lin, Y. 3D Printed Integrated Sensors: From Fabrication to Applications—A Review. *Nanomaterials* **2023**, *13*, 3148, doi:10.3390/nano13243148.
81. Biserova-Tahchieva, A.; Biezma-Moraleda, M.V.; Llorca-Isern, N.; Gonzalez-Lavin, J.; Linhardt, P. Additive Manufacturing Processes in Selected Corrosion Resistant Materials: A State of Knowledge Review. *Materials* **2023**, *16*, 1893, doi:10.3390/ma16051893.

82. Yang, T.; Mazumder, S.; Jin, Y.; Squires, B.; Sofield, M.; Pantawane, M.V.; Dahotre, N.B.; Neogi, A. A Review of Diagnostics Methodologies for Metal Additive Manufacturing Processes and Products. *Materials* **2021**, *14*, 4929, doi:10.3390/ma14174929.
83. Dutta, B.; Babu, S.; Jared, B. Additive Manufacturing Technology. In *Science, Technology and Applications of Metals in Additive Manufacturing*; Elsevier, 2019; pp. 11–53 ISBN 978-0-12-816634-5.
84. Armstrong, M.; Mehrabi, H.; Naveed, N. An Overview of Modern Metal Additive Manufacturing Technology. *Journal of Manufacturing Processes* **2022**, *84*, 1001–1029, doi:10.1016/j.jmapro.2022.10.060.
85. Dass, A.; Moridi, A. State of the Art in Directed Energy Deposition: From Additive Manufacturing to Materials Design. *Coatings* **2019**, *9*, 418, doi:10.3390/coatings9070418.
86. Dutta, B.; Froes, F.H. The Additive Manufacturing of Titanium Alloys. In *Additive Manufacturing of Titanium Alloys*; Elsevier, 2016; pp. 1–10 ISBN 978-0-12-804782-8.
87. Wang, J.; Tang, L.; Xue, Y.; Zhao, Z.; Ye, Z.; Cao, W.; Zhu, J.; Jiang, F. Microstructure and Properties of (Diamond + TiC) Reinforced Ti6Al4V Titanium Matrix Composites Manufactured by Directed Energy Deposition. *Journal of Materials Research and Technology* **2024**, *28*, 3110–3120, doi:10.1016/j.jmrt.2023.12.227.
88. Carroll, B.E.; Palmer, T.A.; Beese, A.M. Anisotropic Tensile Behavior of Ti–6Al–4V Components Fabricated with Directed Energy Deposition Additive Manufacturing. *Acta Materialia* **2015**, *87*, 309–320, doi:10.1016/j.actamat.2014.12.054.
89. Qiu, C.; Ravi, G.A.; Dance, C.; Ranson, A.; Dilworth, S.; Attallah, M.M. Fabrication of Large Ti–6Al–4V Structures by Direct Laser Deposition. *Journal of Alloys and Compounds* **2015**, *629*, 351–361, doi:10.1016/j.jallcom.2014.12.234.
90. Razavi, N.; Bordonaro, G.; Ferro, P.; Torgersen, J.; Berto, F. Porosity Effect on Tensile Behavior of Ti-6Al-4V Specimens Produced by Laser Engineered Net Shaping Technology. *Proceedings of the Institution of Mechanical Engineers, Part C: Journal of Mechanical Engineering Science* **2021**, *235*, 1930–1937, doi:10.1177/0954406218813384.
91. Byun, Y.; Lee, S.; Seo, S.-M.; Yeom, J.; Kim, S.E.; Kang, N.; Hong, J. Effects of Cr and Fe Addition on Microstructure and Tensile Properties of Ti–6Al–4V Prepared by Direct Energy Deposition. *Met. Mater. Int.* **2018**, *24*, 1213–1220, doi:10.1007/s12540-018-0148-x.
92. Svetlizky, D.; Das, M.; Zheng, B.; Vyatskikh, A.L.; Bose, S.; Bandyopadhyay, A.; Schoenung, J.M.; Lavernia, E.J.; Eliaz, N. Directed Energy Deposition (DED) Additive Manufacturing: Physical Characteristics, Defects, Challenges and Applications. *Materials Today* **2021**, *49*, 271–295, doi:10.1016/j.mattod.2021.03.020.
93. Ma, H.Y.; Wang, J.C.; Qin, P.; Liu, Y.J.; Chen, L.Y.; Wang, L.Q.; Zhang, L.C. Advances in Additively Manufactured Titanium Alloys by Powder Bed Fusion and Directed Energy Deposition: Microstructure, Defects, and Mechanical Behavior. *Journal of Materials Science & Technology* **2024**, *183*, 32–62, doi:10.1016/j.jmst.2023.11.003.
94. Oh, H.; Lee, J.; Kim, J.G.; Kim, S. Effect of Defects on Environment-Assisted Fracture (EAF) Behavior of Ti–6Al–4V Alloy Fabricated by Direct Energy Deposition (DED). *Journal of Materials Research and Technology* **2022**, *20*, 4365–4377, doi:10.1016/j.jmrt.2022.08.158.
95. Laleh, M.; Sadeghi, E.; Revilla, R.I.; Chao, Q.; Haghdadi, N.; Hughes, A.E.; Xu, W.; De Graeve, I.; Qian, M.; Gibson, I.; et al. Heat Treatment for Metal Additive Manufacturing. *Progress in Materials Science* **2023**, *133*, 101051, doi:10.1016/j.pmatsci.2022.101051.
96. Mostafaei, A.; Zhao, C.; He, Y.; Reza Ghiaasiaan, S.; Shi, B.; Shao, S.; Shamsaei, N.; Wu, Z.; Kouraytem, N.; Sun, T.; et al. Defects and Anomalies in Powder Bed Fusion Metal Additive Manufacturing. *Current Opinion in Solid State and Materials Science* **2022**, *26*, 100974, doi:10.1016/j.cossms.2021.100974.
97. Świetlicki, A.; Walczak, M.; Szala, M. Effect of Shot Peening on Corrosion Resistance of Additive Manufactured 17-4PH Steel. *Materials Science-Poland* **2022**, *40*, 135–151, doi:10.2478/msp-2022-0038.
98. Żebrowski, R.; Walczak, M.; Korga, A.; Iwan, M.; Szala, M. Effect of Shot Peening on the Mechanical Properties and Cytotoxicity Behaviour of Titanium Implants Produced by 3D Printing Technology. *Journal of Healthcare Engineering* **2019**, *2019*, 1–11, doi:10.1155/2019/8169538.
99. Avcu, E.; Abakay, E.; Yıldıran Avcu, Y.; Çalım, E.; Gökalp, İ.; Iakovakis, E.; Koç, F.G.; Yamanoglu, R.; Akıncı, A.; Guney, M. Corrosion Behavior of Shot-Peened Ti6Al4V Alloy Produced via Pressure-Assisted Sintering. *Coatings* **2023**, *13*, 2036, doi:10.3390/coatings13122036.
100. Żebrowski, R.; Walczak, M. Effect of the shot peening on surface properties and tribological performance of Ti-6Al-4V alloy produced by means of DMLS technology. *Archives of Metallurgy and Materials* **2019**, doi:10.24425/amm.2019.126263.
101. Ganesh, B.K.C.; Sha, W.; Ramanaiah, N.; Krishnaiah, A. Effect of Shotpeening on Sliding Wear and Tensile Behavior of Titanium Implant Alloys. *Materials & Design (1980-2015)* **2014**, *56*, 480–486, doi:10.1016/j.matdes.2013.11.052.
102. Li, D.; Chen, H.N.; Xu, H. The Effect of Nanostructured Surface Layer on the Fatigue Behaviors of a Carbon Steel. *Applied Surface Science* **2009**, *255*, 3811–3816, doi:10.1016/j.apsusc.2008.10.037.
103. Lv, Y.; Lei, L.; Sun, L. Effect of Shot Peening on the Fatigue Resistance of Laser Surface Melted 20CrMnTi Steel Gear. *Materials Science and Engineering: A* **2015**, *629*, 8–15, doi:10.1016/j.msea.2015.01.074.

104. Lv, Y.; Lei, L.; Sun, L. Influence of Different Combined Severe Shot Peening and Laser Surface Melting Treatments on the Fatigue Performance of 20CrMnTi Steel Gear. *Materials Science and Engineering: A* **2016**, *658*, 77–85, doi:10.1016/j.msea.2016.01.050.
105. Azar, V.; Hashemi, B.; Rezaee Yazdi, M. The Effect of Shot Peening on Fatigue and Corrosion Behavior of 316L Stainless Steel in Ringer's Solution. *Surface and Coatings Technology* **2010**, *204*, 3546–3551, doi:10.1016/j.surfcoat.2010.04.015.
106. Xie, B.; Gao, K. Research Progress of Surface Treatment Technologies on Titanium Alloys: A Mini Review. *Coatings* **2023**, *13*, 1486, doi:10.3390/coatings13091486.
107. Xie, L.; Jiang, C.; Lu, W. The Influence of Shot Peening on the Surface Properties of (TiB+TiC)/Ti–6Al–4V. *Applied Surface Science* **2013**, *280*, 981–988, doi:10.1016/j.apsusc.2013.05.135.
108. Xie, L.; Jiang, C.; Lu, W.; Zhan, K.; Chen, Y. Investigation on the Residual Stress and Microstructure of (TiB+TiC)/Ti–6Al–4V Composite after Shot Peening. *Materials Science and Engineering: A* **2011**, *528*, 3423–3427, doi:10.1016/j.msea.2011.01.022.
109. Petit-Renaud, F. Optimization of the Shot Peening Parameters. In *Shot Peening*; Wagner, L., Ed.; Wiley, 2003; pp. 119–129 ISBN 978-3-527-60658-0.
110. Żebrowski, R.; Walczak, M.; Klepka, T.; Pasierbiewicz, K. Effect of the Shot Peening on Surface Properties of Ti-6Al-4V Alloy Produced by Means of DMLS Technology. *Eksploatacja i Niezawodność – Maintenance and Reliability* **2019**, *21*, 46–53, doi:10.17531/ein.2019.1.6.
111. Żebrowski, R.; Walczak, M. The Effect of Shot Peening on the Corrosion Behaviour of Ti-6Al-4V Alloy Made by DMLS. *Advances in Materials Science* **2018**, *18*, 43–54, doi:10.1515/adms-2017-0040.
112. Ongtrakulkij, G.; Khantachawana, A.; Kondoh, K. Effects of Media Parameters on Enhance Ability of Hardness and Residual Stress of Ti6Al4V by Fine Shot Peening. *Surfaces and Interfaces* **2020**, *18*, 100424, doi:10.1016/j.surfin.2019.100424.
113. Jelliti, S.; Richard, C.; Retraint, D.; Roland, T.; Chemkhi, M.; Demangel, C. Effect of Surface Nanocrystallization on the Corrosion Behavior of Ti–6Al–4V Titanium Alloy. *Surface and Coatings Technology* **2013**, *224*, 82–87, doi:10.1016/j.surfcoat.2013.02.052.
114. Kameyama, Y.; Komotori, J. Effect of Micro Ploughing during Fine Particle Peening Process on the Microstructure of Metallic Materials. *Journal of Materials Processing Technology* **2009**, *209*, 6146–6155, doi:10.1016/j.jmatprotec.2009.08.010.
115. Yıldıran Avcu, Y.; Yetik, O.; Guney, M.; Iakovakis, E.; Sınmazçelik, T.; Avcu, E. Surface, Subsurface and Tribological Properties of Ti6Al4V Alloy Shot Peened under Different Parameters. *Materials* **2020**, *13*, 4363, doi:10.3390/ma13194363.
116. Faria, A.C.L.; Rodrigues, R.C.S.; Claro, A.P.R.A.; De Mattos, M.D.G.C.; Ribeiro, R.F. Wear Resistance of Experimental Titanium Alloys for Dental Applications. *Journal of the Mechanical Behavior of Biomedical Materials* **2011**, *4*, 1873–1879, doi:10.1016/j.jmbbm.2011.06.004.
117. Airao, J.; Kishore, H.; Nirala, C.K. Comparative Analysis of Tool Wear in Micro-Milling of Wrought and Selective Laser Melted Ti6Al4V. *Wear* **2023**, *523*, 204788, doi:10.1016/j.wear.2023.204788.
118. Saji, V.S.; Choe, H.-C. Electrochemical Behavior of Co-Cr and Ni-Cr Dental Cast Alloys. *Transactions of Nonferrous Metals Society of China* **2009**, *19*, 785–790, doi:10.1016/S1003-6326(08)60350-7.
119. Saji, V.S.; Choe, H.C. Preferential Dissolution Behaviour in Ni-Cr Dental Cast Alloy. *Bull Mater Sci* **2010**, *33*, 463–468, doi:10.1007/s12034-010-0071-3.
120. Coelho, L.B.; Kossman, S.; Mejias, A.; Noirfalise, X.; Montagne, A.; Van Gorp, A.; Poorteman, M.; Olivier, M.-G. Mechanical and Corrosion Characterization of Industrially Treated 316L Stainless Steel Surfaces. *Surface and Coatings Technology* **2020**, *382*, 125175, doi:10.1016/j.surfcoat.2019.125175.
121. Ahmed, A.A.; Mhaede, M.; Wollmann, M.; Wagner, L. Effect of Micro Shot Peening on the Mechanical Properties and Corrosion Behavior of Two Microstructure Ti–6Al–4V Alloy. *Applied Surface Science* **2016**, *363*, 50–58, doi:10.1016/j.apsusc.2015.12.019.
122. Bagherifard, S.; Ghelichi, R.; Guagliano, M. Numerical and Experimental Analysis of Surface Roughness Generated by Shot Peening. *Applied Surface Science* **2012**, *258*, 6831–6840, doi:10.1016/j.apsusc.2012.03.111.
123. Yi, R.; Ji, J.; Zhan, Z.; Deng, H. Mechanism Study of Electropolishing from the Perspective of Etching Isotropy. *Journal of Materials Processing Technology* **2022**, *305*, 117599, doi:10.1016/j.jmatprotec.2022.117599.
124. Landolt, D. Fundamental Aspects of Electropolishing. *Electrochimica Acta* **1987**, *32*, 1–11, doi:10.1016/0013-4686(87)87001-9.
125. Datta, M.; Landolt, D. Fundamental Aspects and Applications of Electrochemical Microfabrication. *Electrochimica Acta* **2000**, *45*, 2535–2558, doi:10.1016/S0013-4686(00)00350-9.
126. Saito, K. Development of Electropolishing Technology for Superconducting Cavities. In Proceedings of the Proceedings of the 2003 Bipolar/BiCMOS Circuits and Technology Meeting (IEEE Cat. No.03CH37440); IEEE: Portland, OR, USA, 2003; pp. 462–466.
127. Hensel, K.B. Electropolishing. *Metal Finishing* **1999**, *97*, 440–448, doi:10.1016/S0026-0576(00)83104-9.

128. Wynick, G.L.; Boehlert, C.J. Use of Electropolishing for Enhanced Metallic Specimen Preparation for Electron Backscatter Diffraction Analysis. *Materials Characterization* **2005**, *55*, 190–202, doi:10.1016/j.matchar.2005.04.008.
129. Wang, Y.; Wei, X.; Li, Z.; Jing, X.; Gong, Z.; Liu, C. Surface Performance and Optimization of Nickel Titanium Alloy Electropolishing Parameters. *International Journal of Electrochemical Science* **2021**, *16*, 210745, doi:10.20964/2021.07.23.
130. Yang, G.; Wang, B.; Tawfiq, K.; Wei, H.; Zhou, S.; Chen, G. Electropolishing of Surfaces: Theory and Applications. *Surface Engineering* **2017**, *33*, 149–166, doi:10.1080/02670844.2016.1198452.
131. Zhang, Y.; Jianzhong, L.I.; Che, S. Electropolishing Mechanism of Ti-6Al-4V Alloy Fabricated by Selective Laser Melting. *International Journal of Electrochemical Science* **2018**, *13*, 4792–4807, doi:10.20964/2018.05.79.
132. Mathieu, J.B.; Landolt, D. Electropolishing of Titanium in Perchloric Acid-Acetic Acid Solution: II . Polarization Behavior and Stoichiometry. *J. Electrochem. Soc.* **1978**, *125*, 1044–1049, doi:10.1149/1.2131618.
133. Peighambardoust, N.-S.; Nasirpouri, F. Electropolishing Behaviour of Pure Titanium in Perchloric Acid–Methanol–Ethylene Glycol Mixed Solution. *Transactions of the IMF* **2014**, *92*, 132–139, doi:10.1179/0020296713Z.000000000135.
134. Piotrowski, O.; Madore, C.; Landolt, D. The Mechanism of Electropolishing of Titanium in Methanol-Sulfuric Acid Electrolytes. *J. Electrochem. Soc.* **1998**, *145*, 2362–2369, doi:10.1149/1.1838644.
135. Kim, D.; Son, K.; Sung, D.; Kim, Y.; Chung, W. Effect of Added Ethanol in Ethylene Glycol–NaCl Electrolyte on Titanium Electropolishing. *Corrosion Science* **2015**, *98*, 494–499, doi:10.1016/j.corsci.2015.05.057.
136. Smith, E.L.; Abbott, A.P.; Ryder, K.S. Deep Eutectic Solvents (DESs) and Their Applications. *Chem. Rev.* **2014**, *114*, 11060–11082, doi:10.1021/cr300162p.
137. Holze, R. Electrodeposition from Ionic Liquids. F. Endres, A. P. Abbott, and D. R. MacFarlane (Eds). WILEY-VCH, Weinheim, 2008: 387 + XXII p., 105 €; ISBN 978-3-52731565-9. *J Solid State Electrochem* **2009**, *13*, 1633–1634, doi:10.1007/s10008-009-0821-6.
138. Jhong, Y.-T.; Chao, C.-Y.; Hung, W.-C.; Du, J.-K. Effects of Various Polishing Techniques on the Surface Characteristics of the Ti-6Al-4V Alloy and on Bacterial Adhesion. *Coatings* **2020**, *10*, 1057, doi:10.3390/coatings10111057.
139. Han, X.; Ma, J.; Tian, A.; Wang, Y.; Li, Y.; Dong, B.; Tong, X.; Ma, X. Surface Modification Techniques of Titanium and Titanium Alloys for Biomedical Orthopaedics Applications: A Review. *Colloids and Surfaces B: Biointerfaces* **2023**, *227*, 113339, doi:10.1016/j.colsurfb.2023.113339.
140. Kityk, A.; Švec, P.; Šoltys, J.; Pavlik, V.; Hnatko, M. Deep inside of the Mechanism of Electrochemical Surface Etching of α + β Ti6Al4V Alloy in Room-Temperature Deep Eutectic Solvent Ethaline. *Journal of Molecular Liquids* **2023**, *375*, 121316, doi:10.1016/j.molliq.2023.121316.
141. Antonini, L.M.; Mielczarski, R.G.; Pigatto, C.; Müller, I.L.; Malfatti, C.D.F. The Influence of the Operating Parameters of Titanium Electropolishing to Obtain Nanostructured Titanium Surfaces. *MSF* **2012**, *727–728*, 1638–1642, doi:10.4028/www.scientific.net/MSF.727-728.1638.
142. Guo, P.; Zhao, Y.; Zeng, W.; Hong, Q. The Effect of Microstructure on the Mechanical Properties of TC4-DT Titanium Alloys. *Materials Science and Engineering: A* **2013**, *563*, 106–111, doi:10.1016/j.msea.2012.11.033.
143. Velmurugan, C.; Senthilkumar, V.; Sarala, S.; Arivarasan, J. Low Temperature Diffusion Bonding of Ti-6Al-4V and Duplex Stainless Steel. *Journal of Materials Processing Technology* **2016**, *234*, 272–279, doi:10.1016/j.jmatprotec.2016.03.013.
144. Zammit, A.; Bonnici, M.; Mhaede, M.; Wan, R.; Wagner, L. Shot Peening of Austempered Ductile Iron Gears. *Surface Engineering* **2017**, *33*, 679–686, doi:10.1080/02670844.2016.1266118.
145. Avsec, K.; Jenko, M.; Conradi, M.; Kocijan, A.; Vesel, A.; Kovač, J.; Godec, M.; Belič, I.; Šetina Batič, B.; Donik, Č.; et al. Surface Properties of Retrieved Cementless Femoral Hip Endoprostheses Produced from a Ti6Al7Nb Alloy. *Coatings* **2019**, *9*, 868, doi:10.3390/coatings9120868.
146. Lopez-Ruiz, P.; Garcia-Blanco, M.B.; Vara, G.; Fernández-Pariente, I.; Guagliano, M.; Bagherifard, S. Obtaining Tailored Surface Characteristics by Combining Shot Peening and Electropolishing on 316L Stainless Steel. *Applied Surface Science* **2019**, *492*, 1–7, doi:10.1016/j.apsusc.2019.06.042.
147. Kiel, M.; Szewczenko, J.; Marciniak, J.; Nowińska, K. Electrochemical Properties of Ti-6Al-4V ELI Alloy after Anodization. In *Information Technologies in Biomedicine*; Piętka, E., Kawa, J., Eds.; Lecture Notes in Computer Science; Springer Berlin Heidelberg: Berlin, Heidelberg, 2012; Vol. 7339, pp. 369–378 ISBN 978-3-642-31195-6.
148. Kiel-Jamrozik, M.; Szewczenko, J.; Basiaga, M.; Nowińska, K. Technological Capabilities of Surface Layers Formation on Implant Made of Ti-6Al-4V Eli Alloy. *Acta of Bioengineering and Biomechanics; 01/2015; ISSN 1509-409X* **2015**, doi:10.5277/ABB-00065-2014-03.

 doi:10.20944/preprints202401.1375.v1

149. Pochrząst, M.; Marciniak, J.; Szewczenko, J.; Walke, W. Application of Electrochemical Impedance Spectroscopy for Comparison Analysis of Surface Modified Ti-6Al-4V ELI and Ti-6Al-7Nb Alloys. In *Information Technologies in Biomedicine*; Piętka, E., Kawa, J., Eds.; Lecture Notes in Computer Science; Springer Berlin Heidelberg: Berlin, Heidelberg, 2012; Vol. 7339, pp. 379–388 ISBN 978-3-642-31195-6.
150. Szewczenko, J.; Walke, W.; Nowinska, K.; Marciniak, J. Corrosion Resistance of Ti-6Al-4V Alloy after Diverse Surface Treatments. *Materialwissenschaft Werkst* **2010**, *41*, 360–371, doi:10.1002/mawe.201000610.